DISTRIBUTED GENERATION WITH SOFC & CAES TECHNOLOGIES

LOAD-FOLLOWING HEAT, HOT WATER & POWER DISTRIBUTED GENERATION USING AN INTEGRATED SOLID OXIDE FUEL CELL, COMPRESSED AIR ENERGY STORAGE AND SOLAR PANEL ARRAY SYSTEM

By KYLE LEFEBVRE, B.Eng.Biosci

A Thesis Submitted to the School of Graduate Studies

in Partial Fulfilment of the Requirements

for the Degree

Master of Applied Science

McMaster University

MASTER OF APPLIED SCIENCE (2015) McMaster University

(Chemical Engineering) Hamilton, Ontario, Canada

TITLE: Load-following Heat, Hot Water & Power Distributed Generation Using an Integrated Solid Oxide Fuel Cell, Compressed Air Energy Storage and Solar Panel Array System

AUTHOR: Kyle Lefebvre

B.Eng.Biosci (McMaster University)

SUPERVISOR: Dr. Thomas A. Adams II

NUMBER OF PAGES: xvi, 86

Lay Abstract

With growing concerns for the negative impact humans have on the environment, research has turned to reform the power production industry, and to look at the potential of generating power at the point of use. This thesis investigates the potential benefits of combining fuel cells and energy storage technologies to provide heat, hot water, and power for a single building. The system was found to provide the majority of heat (upwards of 75%), hot water, and power (upwards of 94%) demanded by the building over the course of a year, while also reducing the CO_2 emissions associated with the building by upwards of 27% compared to the current state-of-the-art technologies. The system is costly (21% to 150% greater) compared to current market prices for electricity; however it is significantly less expensive compared to alternative on-site generation technologies.

Abstract

Distributed generation (defined as the production of power in small quantities at the point of use) has recently gained significant interest due to its benefits over a centralized approach. This thesis investigates the integration of a natural gas fed solid-oxide fuel cell (SOFC) and compressed air energy storage (CAES) technologies for distributed generation at the building-level scale. The SOFC/CAES system is also integrated with multiple vital sub-systems (including on-site solar panels) for the building to provide the heat, through an in-floor heating system, hot water, and power demanded by the building. This thesis investigates the models for the SOFC/CAES system, and implements them in a generic analysis tool providing a means for rapid analysis of a wide variety of case studies. The analysis tool determines the ability of the SOFC/CAES system to follow the power and heat loads demanded by the building, and evaluates its performance with an assortment of metrics, including efficiencies, CO_2 emissions and grid-independence. The SOFC/CAES system was investigated for the new ExCEL building at McMaster University. It was found that the system was able to produce upwards 75% of the heat and hot water demand, and upwards of 94% of the power demand of the building. When compared to the current state-of-the-art natural gas based power producing technology and high efficiency furnace, the SOFC/CAES system reduces the CO_2 emissions associated with the building by a minimum of 8.7% and a maximum of 26.95%. The cost of electricity for the system is significantly (21% to 150%) more costly than current

market prices; however the SOFC/CAES system is the least costly of all other distributed generation technologies investigated for the case of the ExCEL building.

Acknowledgements

I would firstly like to thank my supervisor, Dr. Adams, for all of his advisement during my degree. All of his aid in my project is enough to make him a good supervisor, but it’s his strive to make me and all his other students comfortable that makes him great. I appreciate all he did for me, and I am glad to have had an advisor, a boss, a friend, and a lead for my curling team all in one.

Secondly, I would like to thank all the other students who have simultaneously been my friends, teammates and mentors. I would like to specifically acknowledge those in the Chem Eng Grad Student Society with me for the past couple years, namely Jake, Daryl, Scott, Trevor, and Patrick. The odd mix of serious conversations and tomfoolery has been appreciated and will be sorely missed.

Finally, I would like to thank my family for their support throughout the past couple of years. My parents have always encouraged me to pursue what I felt was best for me, and I never would have taken this opportunity if it weren’t for them. Thanks also go to my siblings for giving me some much needed breaks from my academic life, keeping my ego in check and never hesitating to help me with anything I needed.

Thank you everyone, including those I didn’t have space to fit in here, for everything you have done for me.

Table of Contents

List of Figures

List of Tables

Chapter 4

Chapter 5

List of Abbreviations and Symbols

Abbreviations

AC	alternating current
CAES	compressed air energy storage
CCS	carbon capture and sequestration
CHP	combined heat and power
COE	cost of electricity
COH	cost of heat
DC	direct current
DOE	department of energy
DG	distributed generation
ExCEL	engineering centre for experiential learning
FOB	free on board
FU	fuel utilization
GUI	graphical user interface
HDH	heating degree hour
HHV	higher heating value
HRSG	heat recovery and steam generation
IEC	international electrotechnical commission
LHV	lower heating value
MCFC	molten carbonate fuel cell

MSFU	modifiable seasonal fuel utilization
NETL	national energy technology laboratory
NGCC	natural gas combined cycle
PFD	process flow diagram
RENES	renewable energy estimator
RHO	rolling horizon optimization
SOFC	solid oxide fuel cell
TAC	total annualized cost
TER	thermal to electric ratio

Symbols

a	model coefficient
F	flow to or from CAES vessel
P	current vessel pressure
W	surrogate model output (heat or power)

Declaration of Academic Achievement

All work presented in this thesis, including program development, data collection, and techno-economic analyses, was performed by myself. Guidance and advice on research directions was provided by Dr. Adams.

Chapter 1

INTRODUCTION

1.1. Motivation

The majority of the total global power supply is produced through the consumption of fossil fuels. Due to growing concerns regarding the impact humans have on the environment, it has become imperative to improve the efficiency of fossil fuel based power production technologies as we transition to a sustainable future for the energy industry. However, the potential areas for improved electricity generation do not end at the gate of the power plant; a significant source of inefficiency in the current power grid (aside from technical limitations) is due to the lengthy transmission distances from the power plant to the consumer (IEC, 2007). The International Electrotechnical Commission (IEC) predicts these transmission losses to be between 8% and 15%, depending on the distance between the user and the centralized power station, which drastically lowers the overall efficiency of power production (IEC, 2007).

Taking these concerns into account, this work investigates the techno-economic feasibility of the implementation of a solid oxide fuel cell and compressed air energy storage system in the distributed generation of heat, hot water, and power for a small (50 kW average energy demand) building to be constructed on the campus of McMaster University. The efficiency, load-following capabilities, and CO_2 emissions for the proposed system are compared to a standard natural gas combined cycle (NGCC, for the production of power) and high efficiency furnace (to satisfy heat demand). The NGCC is used as the basis for comparison as the NGCC is the current state-of-the-art power producing technology which, like the proposed SOFC/CAES system, uses natural gas as a fuel source. The cost of energy, electricity and heat is compared to other distributed generation technologies to determine where the proposed system stands in the current market.

1.2. Background

1.2.1. Solid oxide fuel cell

A solid oxide fuel cell (SOFC) utilizes electrochemical reactions separated by an impermeable solid oxide barrier, where the oxygen present in air is at the cathode, and the fuel gas is oxidized at the anode, in order to efficiently drive electrons through a load, thereby producing electrical power.

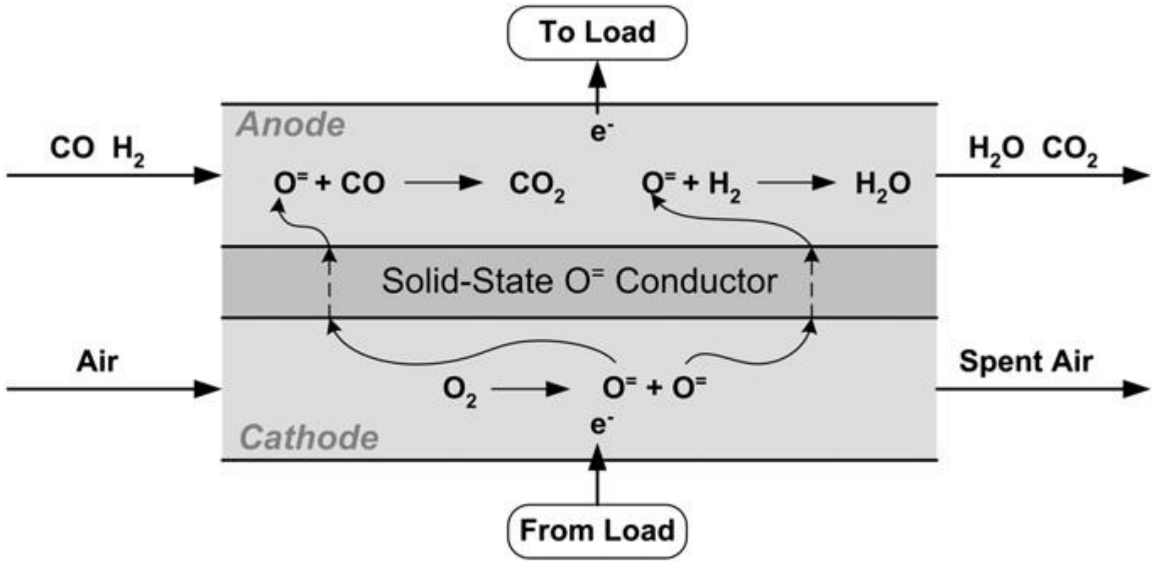

Figure 1.1. Schematic of an SOFC with syngas as a fuel source. Reproduced from (Nease & Adams II, 2013)

SOFCs have been proven to be highly fuel flexible, capable of using methanol (Laosiripojana & Assabumrungat, 2007) and natural gas (Williams, et al., 2005) as direct anodic fuel sources. Additionally, SOFCs can use syngas derived from a wide variety of sources, such as biomass (Nagel, et al., 2009), coal (Williams, et al., 2005), diesel (Williams, et al., 2005), and ethane (Laosiripojana & Assabumrungat, 2007). Previous studies have shown that many kinds of power systems using natural gas fed to a SOFC leads to a reduction in greenhouse gas (GHG) emissions when compared to the state-of-the-art NGCC (Adams II & Barton, 2010), (Adams II, et al., 2012). It has also been proven that, when considering the entire cradle-to-grave life cycle, the megawatt-scale SOFC plants have a much smaller impact on the environment relative to the NGCC (Nease & Adams II, 2014). In addition, the waste heat produced by the SOFC also is at high temperatures (~700-1000°C) (Huijsmans, et al., 1998). Although this adds challenges and cost to the device, it is beneficial from a systems perspective since this high-quality waste heat can be reused for secondary power production or heat and hot water generation.

Although the benefits of SOFCs have been extensively demonstrated, there is a drawback in that operating a SOFC dynamically to follow a load in real time is very difficult in practice due to a significant increase in the risks of SOFC degradation, burner extinguishing, and significant voltage drops due to rapid thermal and current cycling (Stiller, et al., 2006). SOFCs are typically used as base-load power supplies such that the power produced is constant regardless of the time of day or the current demand. This can cause significant overproduction in times of low demand, and significant underproduction in times of peak demand.

1.2.2. Compressed air energy storage

Compressed air energy storage (CAES) is a technology in which power can be stored in the form of elastic potential energy using air compression and expansion. Previous work investigated the potential integration of SOFC and CAES in order to provide load-following capabilities to an SOFC system at the megawatt scale (Nease & Adams II, 2013). The SOFC maintains its base-load operation and, when demand is less than the SOFC capacity, the cathode exhaust from the SOFC is stored in a pressurized cavern by consuming excess base-load power in the CAES compressor train. When the demand exceeds the SOFC capacity, the compressor train is disabled and the stored exhaust is then used to generate power by expanding it to atmospheric conditions through turbines. CAES was chosen as the load-following mechanism due to its synergies with SOFC technologies, namely that the SOFC waste heat can be used to pre-heat the CAES discharge gas prior to turbine expansion. Also, the SOFC exhaust is primarily pressurized nitrogen gas with a small amount of other inert gases mixed in, making it a good candidate for a CAES storage medium. The work found that the SOFC and CAES system was able to closely follow Hamilton's grid power demand loads on an hourly basis while still maintaining high efficiency and very low CO_2 emissions (Nease & Adams II, 2013). The study investigated the application of the integrated SOFC/CAES system at the megawatt scale, and did not assess the ability of the system to provide power on a smaller building scale. Although it may seem a simple task, the megawatt scale study cannot simply be scaled down to the building scale due to many technical and economic limitations, which are discussed further in Chapter 2.

1.2.3. Distributed generation

Distributed generation (DG) is the generation of power in a small scale at the point of use. Many developed countries with low population densities, such as Canada and Russia, have become increasingly decentralized (Ingram, 1998), thereby reducing the demand for bigger centralized power plants and increasing the applicability for decentralized DG. One of the main advantages of DG is that there is the potential for an increase in total system efficiency due to the prevention of transmission losses (Alanne & Saari, 2006). Any potential increases in efficiency promote many benefits, including fewer CO_2 emissions and less fossil fuel depletion per kWh of energy produced (Alanne & Saari, 2006). DG can be applied with many types of power production; however it is typically associated with renewable resources, such as solar panels and wind turbines (Ackermann, et al., 2001). There are many good reasons for using renewables as distributed sources, such as low noise, low maintenance, low environmental impact, high availability, suitability for small scale applications (Nair & Garimella, 2010), and public acceptance (Wolsink, 2012). However, the main issue with renewable sources are that they are extremely inconsistent in their electricity production, and cannot be relied upon at all times (Pepermans, et al., 2005).

There has also been growing interest in using more reliable sources of power for distributed generation. The US Department of Energy (DOE) has contributed a significant amount of funding to the development of fuel cell technology, specifically for the purpose of distributed generation (Williams, et al., 2004). SOFCs and molten carbonate fuel cells (MCFCs) are the main technologies of interest due to their ability to consume natural gas as a fuel source and produce power with high efficiencies. Recent studies by the National Energy Technology Laboratory (NETL) have investigated potential market clients for distributed generation using SOFCs. The NETL determined that there are significant near-term DG opportunities for SOFCs as a primary power source for data centers, as well as backup power sources for office buildings and electrical substations (National Energy Technology Laboratory, 2013). The NETL also identified the potential application of SOFCs for combined heat and power (CHP) generation, namely for commercial and institutional buildings (National Energy Technology Laboratory, 2013).

1.3. Objectives

In this work, we present a system which integrates SOFC and CAES technologies for the load-following distributed generation of heat, hot water, and electric power for a single building. The proposed system may also be integrated with typical DG technologies, such as solar power. The design of such a system is challenging as there exist many constraints for the building scale that do not exist on the megawatt scale. The major constraints to be considered are that the system must be small enough such that it can fit in the maintenance room of the building, operating temperatures must not exceed maximum temperatures set by legislation for indoor piping, and exhaust venting temperatures must be below the maximum discharge temperatures for buildings. These smaller scales and temperatures constraint will likely have a negative effect on system efficiency and cost; however they cannot be ignored as the system is infeasible if the constraints are violated.

The overall research goal is to assess the techno-economic feasibility of the integrated SOFC/CAES system for CHP production, which is achieved through the following steps:

i. Develop a rigorous model in order to determine the operating conditions of the SOFC/CAES system.
ii. Analyze the ability of the SOFC/CAES system to meet the hourly heat and power demand loads on the building scale.

iii. Create a generic analysis tool to allow for a rapid technical analysis of the load-following properties of the system for a wide variety of case studies.

iv. Perform an economic analysis of the proposed system and compare it to other distributed generation technologies to assess the potential application of the SOFC/CAES system.

1.4. Main Contributions

There are two major contributions from this research.

1. **Techno-economic analysis of a novel SOFC/CAES system for load-following CHP** – The technical and economic feasibility of applying an integrated SOFC/CAES system for providing heat, hot water, and power for building on McMaster University is investigated. The effect of different SOFC fuel utilizations (FU) is determined to assess the trade-offs associated with producing different ratios of heat to power. This is the first time that an integrated SOFC/CAES system has been investigated on the small, distributed generation scale.
2. **Development of a general analysis tool –** In this work, an analysis tool is developed to assess the load-following characteristics of the SOFC/CAES system in a generic sense. The tool provides a means to evaluate the feasibility of the system for a wide variety of case studies, whether they are varying operating conditions or different demand profiles.

1.5. Thesis Outline

The thesis is separated into the 5 following chapters:

Chapter 2 – This chapter details the rigorous models, developed in Aspen Plus v8.0, used to determine the heat and power output of the SOFC/CAES system for different operating conditions. The development of surrogate models based on the Aspen Plus simulations is also discussed.

Chapter 3 – This chapter provides comprehensive information on the generic graphical user interface (GUI) analysis tool, developed in Python, used to evaluate the technical feasibility of the SOFC/CAES system. The load-following algorithm and all performance metrics are discussed.

Chapter 4 – This chapter discusses the technical feasibility of applying the SOFC/CAES system for a building on McMaster University. The ability of the system to provide the heat and power demanded by the building is evaluated and compared to current state-of-the-art technologies. The sensitivity of the system's performance to different design decisions is also investigated.

Chapter 5 – The economics of the case studies presented in chapter 5 are discussed in this chapter. The capital and operating costs are analyzed, as well as the cost of energy production for the system, and compared to other DG technologies. The cost trade-offs for the size of the SOFC/CAES system are investigated.

Chapter 6 – The major results and recommendations for future work are provided in this section.

Chapter 2

SOFC AND CAES PROCESS MODELLING

2.1. Introduction

Previous studies have modelled megawatt-scale steady state SOFC/CAES operations using Aspen Plus simulations. However, this works requires modifications to these models as some of the assumptions and components are not practical on a smaller scale. The SOFC and CAES components of the proposed system are modelled after the previous work done by Nease and Adams (Nease & Adams II, 2013), with modifications for small scale applications. The major changes to the model were the redevelopment of the CAES and heat recovery systems, the remodelling of the SOFC model to include internal gas reforming, and the addition of the heat and hot water production systems. The overall integration of all sub-systems is also investigated and is depicted in **Figure 2.1**. A more detailed description of the entire system, and its components, is provided in the following sections.

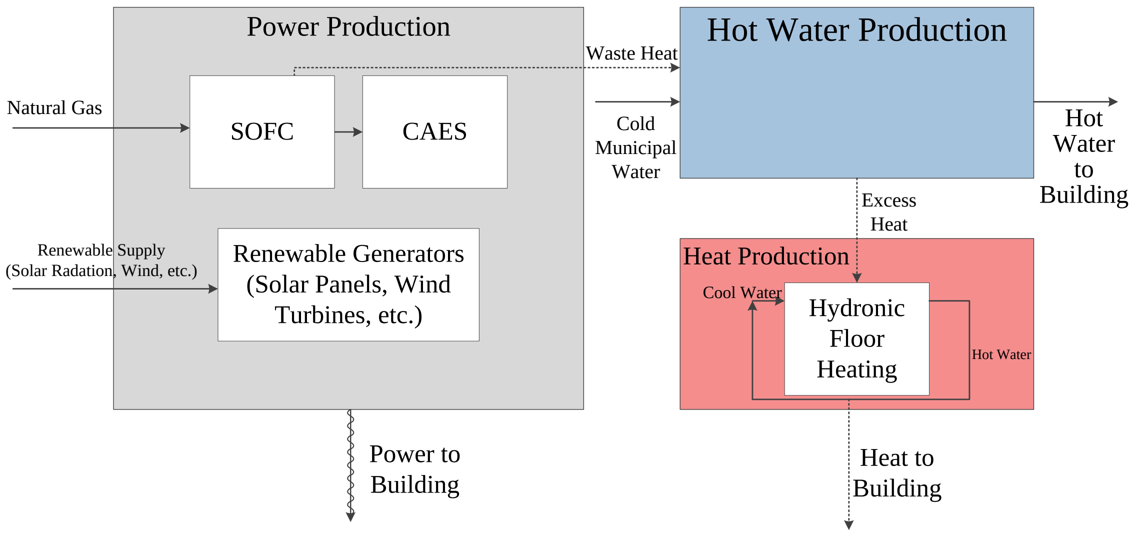

Figure 2.1. Integration of all investigated sub-systems for CHP production

This chapter describes the development of the models used to predict the heat, hot water, and power output of the SOFC/CAES system under varying operating conditions, such as different CAES charging/discharging pressures and flow rates. These models will be used, as discussed in the following chapters, to assess the ability of the system to meet the heat, hot water, and power demand of a building on an hourly basis. The modelling of an integrated SOFC/CAES system at the small scale has never been presented in the open literature, to the best of the author's knowledge.

2.2. Process Models

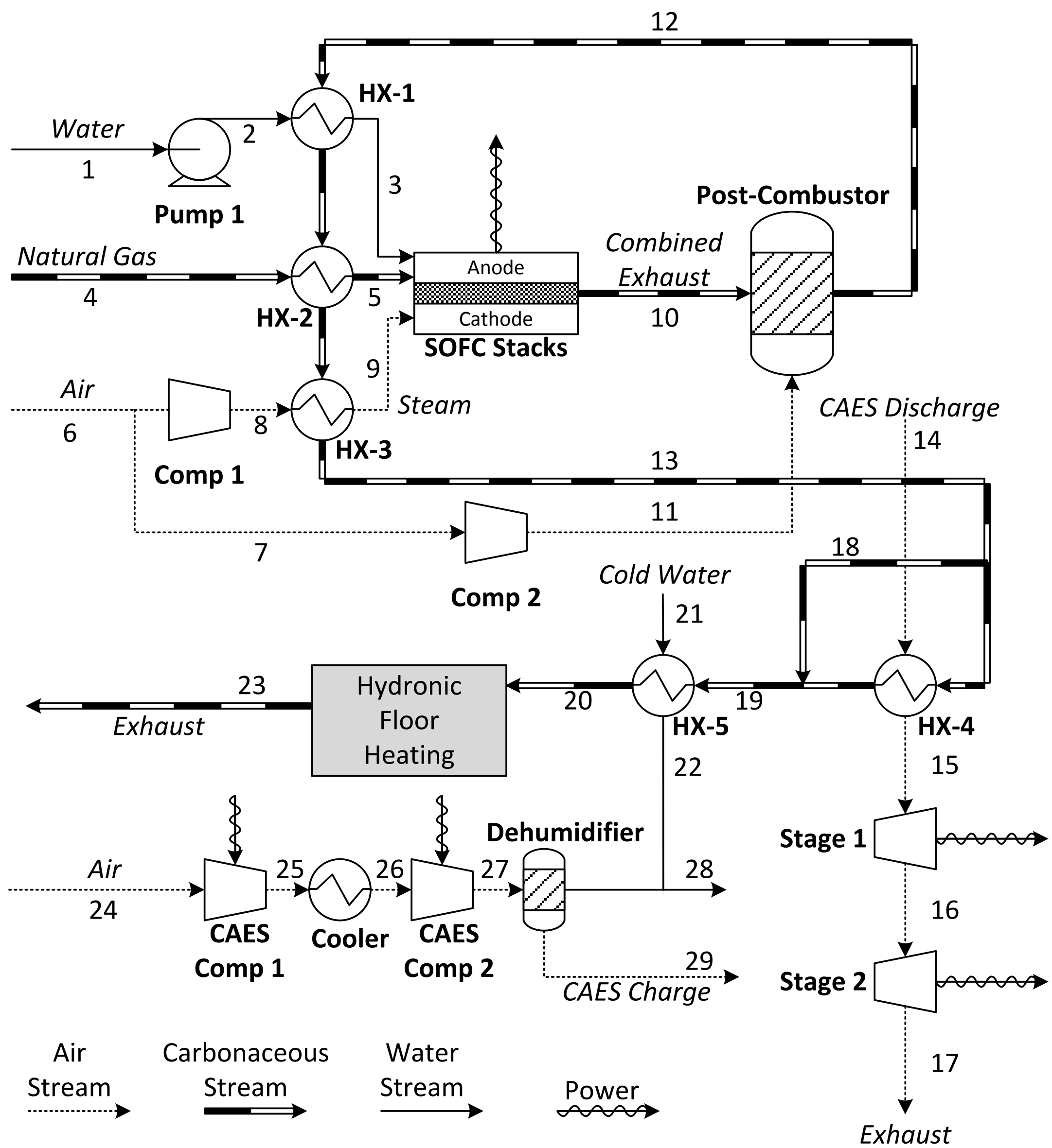

Figure 2.2. Process flow diagram for small scale SOFC/CAES system

The configuration of the integrated SOFC/CAES system for heat, hot water and power production is provided in Figure 2.2. The natural gas is first pre-heated, using recovered heat from the system, and fed to the anode of the SOFC along with steam, also generated from waste heat, to be reformed. Pre-heated air is fed to the cathode of the SOFC and power is produced. The exhausts of the SOFC, along with additional air, are then fed into a post-combustor where the unreacted fuel is consumed to produce heat in the form of hot air. This heat is then used to pre-heat the CAES discharge, if the CAES is discharging, followed by hot water production, and finally to generate heat through a hydronic floor heating system. Additional heat for the hydronic floor heating system is provided by the CAES charging sequence if the CAES is charging. All systems, and their respective models, are provided in detail in the following sections.

2.2.1. Steady state SOFC model

The SOFC model was adapted from Adams and Barton (2010), where details of the model are presented in the "autothermal reforming" case. The SOFC model uses experimental correlations for voltage as a function of pressure and temperature, and considers parameters such as fuel utilization (both 80% and 65% tested in this study), onboard methane reforming, losses associated with DC to AC conversion (4% of power produced) and heat losses to the environment (5% of reaction energy). The SOFC was scaled to a stack power output of 42.5 kW. All steady state models were constructed in Aspen Plus v8.0 using the Peng-Robinson equation of state with the Boston-Mathias modification physical property package, which was shown in the prior work to be suitable for this system.

2.2.1.1. Natural gas reforming

Natural gas is reformed through reactions with steam in order to produce syngas to be used as fuel in the SOFC. The small-scale, commercial SOFCs which are currently available typically operate with internal reforming, where the natural gas is reformed inside the SOFC rather than using an external reforming process (Adams II, et al., 2012). In this work, steam is generated using excess heat from the SOFC, and is fed into the anode of the SOFC along with pre-heated natural gas in order to reform the gas. The model assumes that chemical equilibrium is reached at the operating conditions of the SOFC (800°C and 2.6 bar), resulting in approximately 98% conversion of methane. This requires the assumption that the bulk anode section of the SOFC is well-mixed and there is sufficient residence time for the steam reforming reactions to go to completion.

2.2.1.2. Power and hot water generation

In order to avoid large thermal and pressure gradients in the cell, the SOFC requires the air to be at conditions similar to that of the reformed gas; therefore air is compressed to 2.6 bar and pre-heated to 820°C prior to being fed into the cathode of the SOFC. The exhausts of the SOFC are then combined and fed into an afterburner where, in the presence of additional air, the unreacted fuel combusts to produce heat, as hot air, to be used for heat and hot water generation.

The heat produced by the afterburner is first exchanged with the water feed stream to generate the steam necessary for natural gas reforming. The remaining heat is then used to pre-heat the natural gas and air prior to entering the SOFC. After these steps, any excess heat present in the cathode exhaust stream is passed through a third exchanger in order to generate the necessary amount of hot water demanded by the building.

2.2.1.3. Heat generation

Heat for the building will be provided through hydronic floor heating. Hydronic floor heating provides radiative heat by passing warm water through pipes underneath the floor, where the heat from the water is able to radiate up through the floor and into the building (Olesen, 2002). The system is a closed loop, in that the water flowing through the system is re-heated and recycled in order to maintain building temperature rather than feeding fresh water into the system. A schematic of a hydronic floor system can be seen in Figure 2.3.

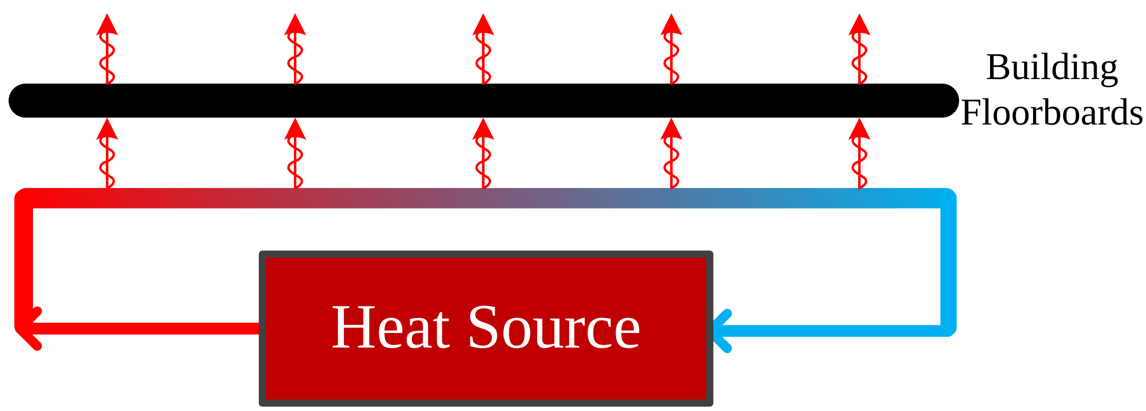

Figure 2.3. Schematic for hydronic floor heating

In this work, the extra heat present in the SOFC exhaust after steam generation, pre-heating, and hot water generation is used to generate as much warm water as possible for the hydronic floor system. The system was designed to cycle between a water temperature of 35°C and 25°C as recommended by the Canada Plan Service for these systems (Canada Plan Service, 2010). After the warm water is produced, the cooled SOFC exhaust is then vented. Although not all heat for the building can be provided by the SOFC at the chosen scale, a significant portion of the demand can be met, as seen in Section 4.4.

2.2.2. Compressed air energy storage model

When the power produced by the SOFC exceeds demand, the surplus electricity is used to compress and store air taken from the surrounding environment. As the air is pressurized, it is also dehumidified in order to avoid complications associated with storing, compressing and expanding water vapour. Compressed air is cooled to the storage temperature of 80°C. A heat exchanger allows the cooling requirement of the CAES charging stream (stream 25 in Figure 2.2) to be provided in colder periods by dispersing the heat to the hydronic floor heating system. This is particularly beneficial because in the winter months the waste heat generated by the SOFC is sometimes insufficient to meet the building demand, and recovering the waste heat generated by compressing air helps mitigate this discrepancy, as seen in Section 4.4.

When the CAES is to be discharged, the stored exhaust must be pre-heated to avoid operational issues with the turbines. The discharge stream is pre-heated to 250°C by the SOFC exhaust prior to the generation of hot water. This results in less heat available for the building heat during times of high electricity demand. The flow rate out of the CAES vessel is determined by a pseudo steady state surrogate model (see Section 2.3) in order to provide the required amount of power. The CAES uses a two-stage microturbine, with pressures of 7.5 bar and 1 bar at the outlet of each stage. This provides a maximum power of 11.5 kW from the CAES discharge train.

The integration of all of these subsystems into a single Aspen Plus simulation allows for computation of the heat and power production of the SOFC/CAES system under various operating conditions, including different CAES discharging and charging conditions.

2.3. Pseudo steady state operation

As previously mentioned, one of the main objectives of this work is to analyze the ability of an integrated SOFC/CAES system to meet the hourly heat and power demand of a building. In order to do this the SOFC/CAES dynamic operating conditions need to be assessed; however the SOFC operation will remain constant, and therefore does not need to be modelled dynamically, and the systems that do change (CAES turbines/compressors, and the hydronic floor heating) all have rapid dynamics that can reach their respective steady states within an hour timeframe. A CAES plant is able to ramp at 10% every 3 seconds while discharging, and ramp at 20% per minute while charging (Fertig & Apt, 2011). Hydronic floor heating has been found to respond to flow rate changes within 15 minutes to remain at a steady state floor temperature (Raftery, et al., 2012). The rapid dynamics of the system allow the hourly dynamic operation of the SOFC/CAES system to be approximated as a series of pseudo steady states to avoid the complexity associated with modelling the dynamics of the SOFC/CAES system. The load-following analysis for the whole year can therefore be performed with 8760 (one per hour of the year) steady state simulations.

The complexity of the Aspen Plus simulation would require upwards of 200 hours of computational time in order to assess the load-following capabilities of the system throughout the year if it were used to determine steady states, which was deemed an unacceptably long amount of time due to the requirement for a variety of case studies for this work. The Aspen Plus simulation was therefore approximated using surrogate models in order to drastically improve the computational time associated with assessing the steady state operating conditions of the SOFC/CAES system.

A series of 48 Aspen Plus simulations were run for both the discharge and charging phases in order to obtain heating and power data for the SOFC/CAES system at different operating conditions. The pressure was varied between 15 bar and 45 bar as these are the assumed operating limits of the vessel. The discharge flow was varied between 0.5 and 15 kmol/hr as these are the minimum (aside from 0) and maximum flow rates for the CAES turbines. The charging flow rate was varied between 0.5 and 4 kmol/hr as higher flow rates violated temperature constraints for the system. The data from the Aspen Plus simulations were fit to non-linear models of the form:

$$W = a_{00} + a_{10}F + a_{01}P + a_{20}F^2 + a_{02}P^2 + a_{11}FP \tag{1}$$

where W is the output of interest (heat or power), F is the flow to (charging phase) or from (discharging phase) the CAES vessel, P is the current pressure in the vessel, and $a_{i,j}$ is the coefficient for *i*th and *j*th power of F and P, respectively.

The eight surrogate models were then each compared to a testing set of 10 different operating conditions to determine the validity of the models. The testing set data were different from the training set (the original 48 simulations) for each model. The surrogate models compared extremely well with the testing sets. The coefficients for the power and heat surrogate models, as well as the R^2 value from the comparison to the testing set, are presented in Table 2.1 and Table 2.2, respectively. This 2^{nd} order form was chosen as a surrogate model of lower order was found to drastically reduce the accuracy of the models. The 2^{nd} order models were found to provide highly accurate, non-spurious predictions of the Aspen Plus models, while higher order models had a negligible effect on model accuracy since the higher order terms had near-zero coefficients. This indicates that the Aspen Plus model has 2^{nd}, and not higher, order characteristics. However, the Aspen Plus model also has more complex nonlinear characteristics (such as exponentials in equilibrium equations) which are not reflected in the surrogate model, and could explain the small error present in the 2^{nd} order surrogate models.

Table 2.1. Surrogate Model Coefficients and R^2 for Power Calculation Models

	Power			
	80 FU		**65 FU**	
	Charging	**Discharging**	**Charging**	**Discharging**
a_{00}	44.56	40.22	44.72	40.13
a_{10}	-2.833	2.269	-3.024	1.1356
a_{01}	-0.136	0.1305	-0.1509	0.3028
a_{20}	0.0001	-0.09356	0.0405	0.00604
a_{02}	0.002092	-0.001522	0.002423	-0.005033
a_{11}	-0.070961	0.0197	-0.08033	0.03574
R^2	0.999	0.972	0.999	0.998

Table 2.2. Surrogate Model Coefficients and R^2 for Heat Calculation Models

	Heat			
	80 FU		**65 FU**	
	Charging	**Discharging**	**Charging**	**Discharging**
a_{00}	14.36	16.02	22.38	23.24
a_{10}	1.037	-0.08899	1.066	-0.4219
a_{01}	0.0403	-0.05177	0.05506	-0.08946
a_{20}	-0.002328	0.04967	-0.01763	-0.002688
a_{02}	-0.0006	0.0005069	-0.00089	0.001594
a_{11}	0.03021	-0.001349	0.03097	-0.01143
R^2	0.995	0.932	0.999	0.994

The surrogate models drastically reduce the computational time required to predict the SOFC/CAES heat and power outputs for a given set of operating conditions. The models are extremely accurate at predicting the testing set, with most models having an R^2 value above 0.99, with a worst case R^2 value of 0.932 occurring in the heat discharge model of the 80% FU system. These models are therefore accurate representations of the Aspen Plus models, and can be used in the analysis tool (see Chapter 3) to provide a rapid study of the technical feasibility of the system.

2.4. Conclusions

In this chapter the models used for the SOFC/CAES integrated system were discussed. An SOFC model based on experimental correlations was combined with a CAES and heat integration simulation, in Aspen Plus v8.0, in order to determine the heat and power output of the SOFC/CAES system when operating under varying conditions. Pseudo steady state surrogate models (one for each heat and power production for both charging and discharging the CAES) were developed, based on the rigorous integrated Aspen Plus model, and were found to be able to accurately and quickly predict the heat and power output of the system. These pseudo steady state models provide the basis for the analysis tool, discussed in the following chapter, to determine the feasibility of the SOFC/CAES integrated system in providing CHP in a small scale application.

Chapter 3

GRAPHICAL USER INTERFACE ANALYSIS TOOL

3.1. Introduction

The previous chapter discussed all the models and simulations used to predict the heat and power output of the SOFC/CAES system, as well as the surrogate models developed from the rigorous Aspen Plus model. This chapter investigates the development of a graphical user interface (GUI) that implements the previously described models in order to determine the load-following properties of the SOFC/CAES system. The GUI is developed as a general tool that is independent of the specific case, and allows for the SOFC/CAES system to be quickly analyzed for a variety of datasets and operating conditions. The user is able to provide hourly heat and power demand profiles, as well as hourly generation profiles from any additional sources of power, such as on-site solar panels or wind turbines. The size and characteristics of the SOFC and CAES systems may also be defined by the user, and after the analysis is complete, performance metrics, such as system efficiencies, grid-independence, and heat generation, are provided to determine the performance of the system.

3.2. Load-following Algorithm

The main purpose of the GUI is to determine the load-following characteristics of a SOFC/CAES system given by the inputs from the user. The load-following algorithm requires data from the user (see Section 3.3.1), including the hourly heat and power demand profiles for the building, the hourly power supplied by any additional (such as renewable) sources, and the sizes and characteristics of the SOFC and CAES systems. The computational sequence for the load-following analysis can be seen in Figure 3.1, and the general strategy is as follows.

At a given time step, assumed to be hourly, the combination of the base-load power from the SOFC and the renewable power supply (as provided by the user) are compared to the current power demand. If the combined power is greater than the demand, the system enters its charging phase, while if the combined power is less than the demand the system enters its discharging phase. The surrogate power models (whether charge or discharge) are then used to determine the CAES flow rate necessary to exactly meet the power demand, and the pressure of the CAES vessel at the next time step is computed based on this flow rate, assuming the air in the CAES vessel behaves as an ideal gas. If the calculated pressure violates a constraint, then the flow rate is set to the maximum allowable value that will not violate a pressure constraint. The CAES air flow rate is then used in the surrogate heat models (whether charge or discharge) to determine the amount of heat produced. It was determined that overproducing heat was unacceptable due to the negative effect on the comfort of the people in the building; therefore if the heat produced by the SOFC/CAES system is greater than the heat demand, the exhaust must be air-cooled in order to avoid safety concerns regarding the temperature of the vented SOFC exhaust streams. This air-cooling provides parasitic power loads associated with blowing the air; therefore the total power demand of the building increases for that particular time step and the previously computed power production is insufficient for the building. Therefore, when air cooling is required, the calculation at that time step is reiterated due to the increased power demand from the parasitic air cooling load. The iteration therefore computes the new flow rate to or from the CAES vessel needed in order to meet the increased power demand (actual building demand + parasitic air-cooling load), and determines if the heat produced, with the previously computed air-cooling, still overproduces heat. If heat is still overproduced, even with the air-cooling, the analysis is once again reiterated at that time step with an additional air-cooling load. This reiteration is performed a maximum of 200 times as more iterations was found to have negligible effects on system performance and was not worth the increase in computation time.

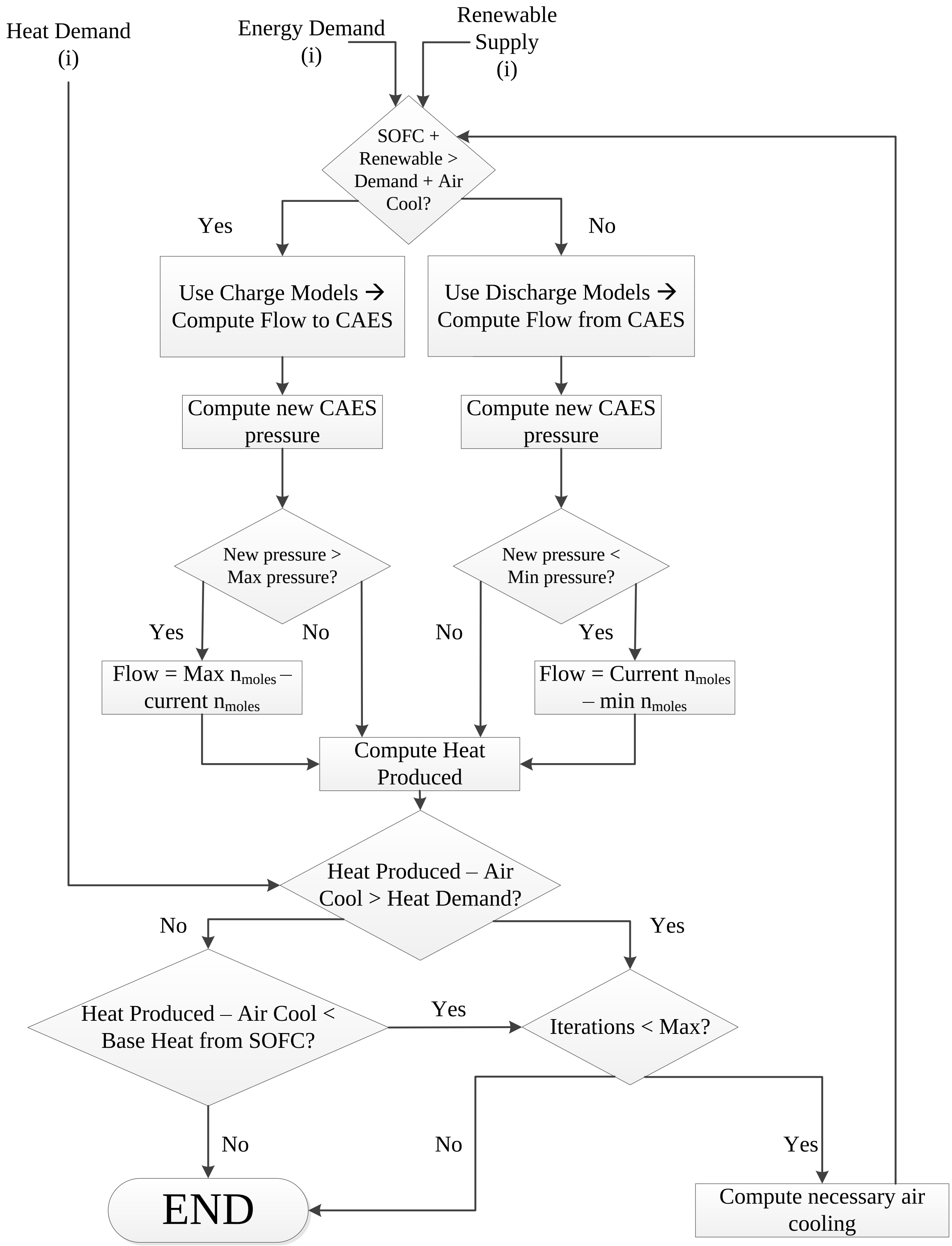

Figure 3.1. Computational algorithm for a single time step of power load-following analysis

For the purpose of this analysis, if the SOFC/CAES system is unable to meet the building power demand, then the deficit is assumed to be provided by the municipal power grid, thereby resulting in indirect CO_2 emissions associated with purchasing the necessary power. Additionally, in the event that excess power is produced by the system and cannot be stored due to the vessel being full, any extra power is delivered back to the grid to displace some of the central grid power. Note that environmental impact of grid electricity will be somewhat different from location to location depending on the mix of power plants which contribute to the power grid in that region. For this study, we have used the CO_2 emissions of an NGCC (Energy Information Administration (EIA), 2012) as the environmental impact of the grid. This allows for a direct comparison between the current centralized use of natural gas (NGCC) and the proposed distributed use of natural gas. It is also a good approximation of a "median" grid as certain provinces, such as Alberta, rely significantly on highly emissive coal based plants, while other provinces, such as British Columbia, rely on minimally emissive hydro-electric plants. In other words, this assumption could result in either an overestimate or an underestimate in the amount of CO_2 emissions attributed to the grid, depending on the location.

If the SOFC/CAES system is unable to meet the heat demand at a given time, the balance is met using a high efficiency furnace, resulting in indirect CO_2 emissions associated with its operation (Energy Information Administration (EIA), 2012). The additional indirect CO_2 emissions from the furnace and centralized power are accounted for in the calculation of total annual CO_2 emissions. The emissions associated with the grid are user-defined by a selection pane (see Section 3.3.6) including a wide variety of possible locations and grid power supply mixtures, such as Alberta, Ontario, BC, US average, and Canada Average. The emissions associated with the furnace are, at the time of writing, embedded in the emission calculations of the GUI and cannot currently be modified by the user.

3.3. GUI Features

The GUI, which is programmed in Python, allows the user to import their specific hourly power and heat demand profiles, as well as any additional power supply from renewable sources, such as on-site solar panels or wind turbines. After the user provides their SOFC and CAES properties, such as size, degradation rate, and fuel utilization, the load-following algorithm is executed and provides a variety of system performance metrics. For an 8760 hour (one year) dataset, the GUI is able to complete the algorithm in less than 30 seconds and provides a comprehensive analysis of the operability and environmental impact of the user-defined system. A screenshot of the GUI is provided in Figure 3.2.

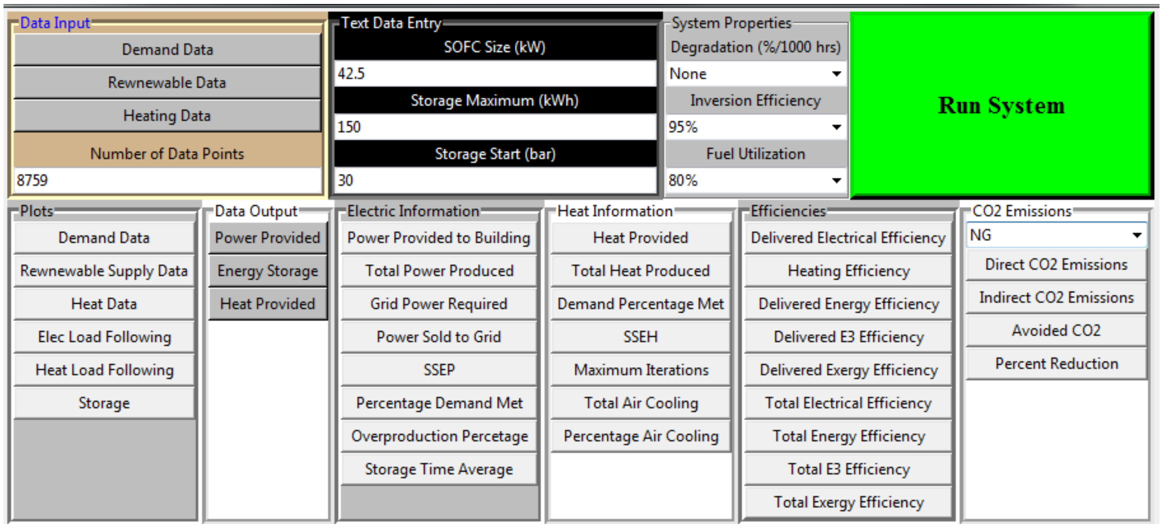

Figure 3.2. Screen shot of the system analysis GUI developed for the proposed system

3.3.1. Data Input, Text Data Entry, and System Properties

The first section of the GUI is the data input section, where the user imports their power demand profile (as prompted when clicking the “Demand Data” button), the power provided by renewable sources (as prompted when clicking the “Renewable Data” button), and their heat demand profile (as prompted when clicking the “Heating Demand” button). In this section, the user also provides the number of data points (in hours) they wish to analyze. The heat and electricity demand files must be imported as Excel files, with 3 columns: Date, Hour, and Hourly Demand. The renewable supply data must also be imported as an Excel file with 3 columns: Date, Hour and Total Hourly Renewable Supply.

The next section of data input is where the user defines the size of the SOFC and CAES for their specific case study. The user is able to type any real number for the SOFC size (in kW), CAES maximum energy storage (in kWh) and starting storage pressure of the vessel (in bar). The values used in these sections are primarily dictated by the magnitude and variability of the power demand profile. A larger average power demand will require a larger SOFC, and a more variable demand profile will require a larger CAES in order to store enough power to meet the large peaks and store enough power during the low valleys.

In the "System Properties" section of the GUI, the user is able to define additional characteristics of the SOFC. The degradation of the SOFC can be selected based on typical degradation rates of SOFCs (0%, 0.1%, 1% and 3% per 1000 hours of operation). The DC to AC inversion efficiency can also be chosen based on the scope of the case study. The fuel utilization (FU) of the SOFC can also be chosen as 80%, 65% or 50%.

Once all of these properties are defined the load-following algorithm can be executed by clicking the "Run System" button or pressing the Enter key, and the ability of the defined SOFC/CAES system, along with the renewable power supply, to meet the provided heat and power demand is evaluated based on a large number of criteria discussed in the following sections.

3.3.2. Plots and Data Output

This section provides a variety of plots in order for the user to visualize the performance of the SOFC/CAES system. The "Demand Data", "Renewable Supply Data" and "Heat Data" buttons provide the plots of the imported data. A sample plot using the "Demand Data" button is provided in Figure 3.3. The "Elec Load Following" and "Heat Load Following" buttons provide the demand profile (in black) plotted alongside the actual electricity and heat delivered by the system (in red). A sample of the "Heat Load Following" plot is provided in Figure 3.4. The "Storage" button provides a plot of the pressure in the storage vessel during the course of the analysis, and a sample is provided in Figure 3.5.

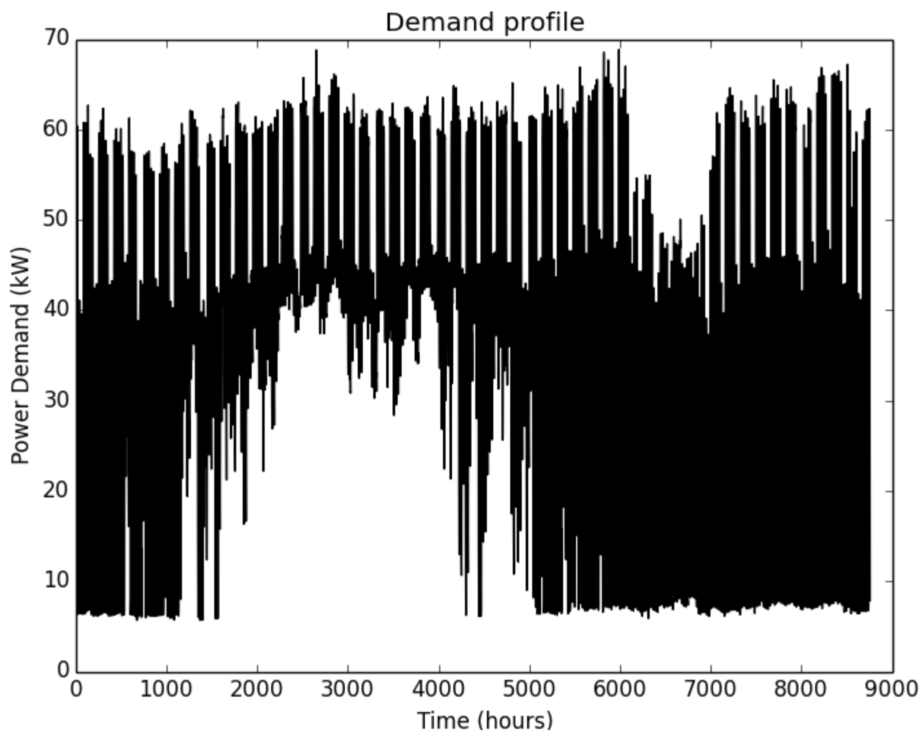

Figure 3.3. Sample of the "Demand Data" plot provided by the GUI

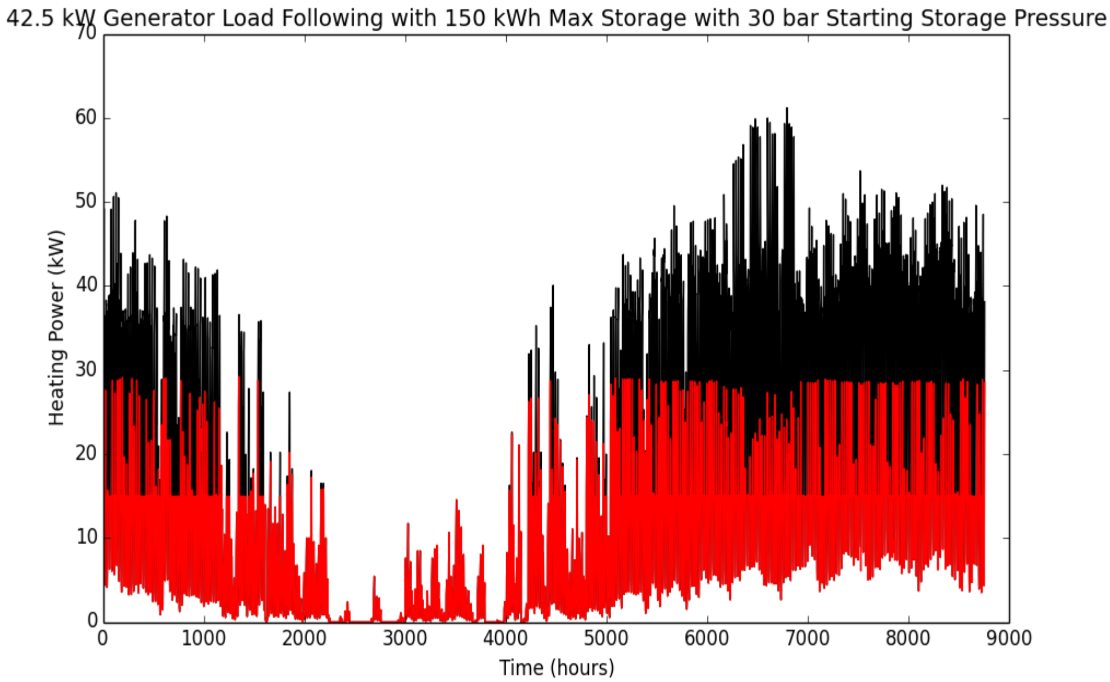

Figure 3.4. Sample of the “Head Load Following” plot provided by the GUI

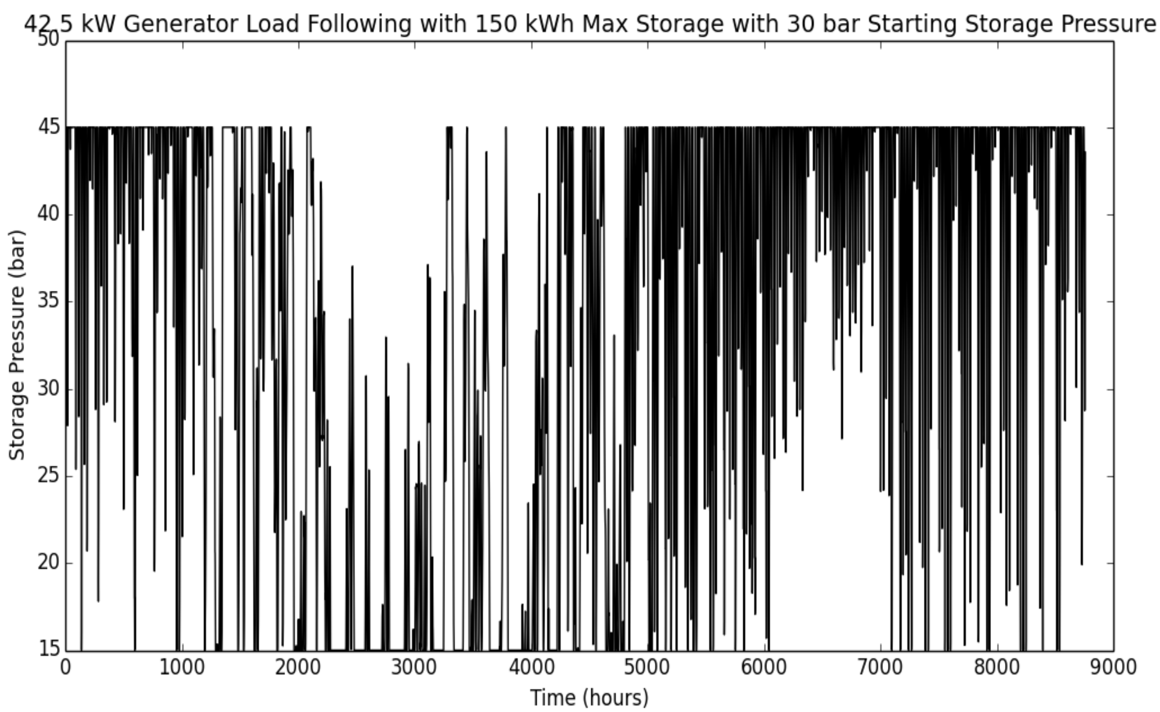

Figure 3.5. Sample of the “Storage” plot provided by the GUI

The “Data Output” section of the GUI provides all the information present in the plots (hourly power provided, heat provided and energy storage) in a .txt file. This allows for the user to export the data if they wish to use it for further analysis, or if they wish to use another program, such as Excel, to generate their own figures.

3.3.3. Electric Information

All of the metrics in the “Electric Information” panel of the GUI are provided as a means for the user to assess the ability of the SOFC/CAES system they have proposed in meeting their power demand profile. The amount of power actually supplied to the building and the total amount of power produced (including overproduction and power used for air cooling in times of heat overproduction) by the system are provided by the “Power Provided to Building” and “Total Power Produced” buttons, respectively. The amount of electricity needed to be purchased from the grid (due to under producing power during peak loads) and the amount of power overproduced that could not be stored in the CAES due to it being full are provided in the “Grid Power Required” and “Power Sold to Grid” buttons, respectively. The “SSEP” button provides the sum of squared error for the electricity load-following, and is computed as follows:

$$SSEP = \sum_{i=1}^{\#\ of\ data\ points} (Power\ Delivered_i - Power\ Demanded_i)^2 \qquad (2)$$

Where the power delivered at each time step is the amount of power supplied to the building by the SOFC/CAES system, and does not include any power that is stored or consumed for air cooling at that time step. A large SSEP indicates a system that is unable to adequately follow the power demand profile, whether it is over-producing, under-producing, or both.

The "Percentage Demand Met", "Overproduction Percentage", and "Storage Time Average" are metrics that gauge whether the SOFC/CAES system is appropriately sized. The percentage demand met is the fraction of the total power demand that is provided by the SOFC/CAES system as opposed to the power that is purchased from the grid. A percentage demand met of 100% indicates that all power is provided by the system and that the building is grid-independent for power, while low (less than 70%) percentage demand met indicates that the SOFC is likely undersized and does not supply an adequate amount of power to the building. Conversely, the "Overproduction Percentage" is the fraction of power produced that cannot be stored due to the CAES being full, and must be sold to the grid. An overproduction percentage of 0% indicates that all power produced is delivered to the building, used for air cooling, or stored for future use. A high overproduction percentage (greater than 30%) indicates that a large fraction of the power produced is not used by the building and is indicative of an oversized SOFC or undersized CAES vessel. The "Storage Time Average" is the fraction of the average CAES vessel pressure throughout the year compared to the maximum CAES vessel pressure. A high (greater than 85%) storage time average indicates that, on average, the CAES vessel is near, or at, full capacity and is therefore likely undersized. Conversely, a low (less than 15%) storage time average indicates that the CAES vessel is, on average, nearly depleted and likely indicates an undersized SOFC.

3.3.4. Heat Information

As with the electric information panel, the “Heat Information” panel provides metrics to the user so that they may assess the ability of their proposed SOFC/CAES system in meeting the provided heat demand profile. The total amount of heat provided to the building and the total amount of heat produced by the system (including the heat needed to be removed via air cooling) are provided by the “Heat Provided” and the “Total Heat Produced” buttons. The “Demand Percentage Met” is the fraction of the total heat demand that is provided by the SOFC/CAES system, with a higher value indicating that more of the heat is provided by the system and therefore less is provided using a furnace. The “SSEH” is the sum of squared error for the heat delivery, and is computed in an identical manner to the SSEP. As with the SSEP, a large SSEH indicates that the system is unable to adequately follow the heat demand profile; however, unlike with the SSEP, this will likely be entirely due to heat underproduction as, with the load-following strategy previously outlined, heat overproduction is undesired and avoided.

The “Total Air Cooling” is the amount of cooling that is required during the course of the simulation, and indicates the total amount of heat overproduction throughout the analysis. The “Percentage Air Cooling” is the fraction of the total air cooling compared to the total amount of heat produced. A high percentage air cooling (greater than 30%) indicates that the SOFC/CAES system is producing a lot of unusable heat and is therefore operating in an extremely inefficient manner. A high percentage air cooling therefore indicates that the SOFC is likely oversized, or needs to operate with a higher FU.

3.3.5. Efficiencies

This section of the GUI provides a variety of efficiency (in both higher heating value, HHV, and lower heating value, LHV) calculations for the SOFC/CAES system. For all calculations, the HHV of the natural gas fuel is assumed to be 14.726 kWh/kg and the LHV is assumed to be 13.095 (Oak Ridge National Laboratory, 2011). The "Delivered Electrical Efficiency" is the fraction of power delivered to the building provided by the SOFC/CAES system (not including any power from the provided renewable supply dataset) compared to the total amount of energy fed into the system as natural gas. This metric therefore indicates the efficiency of the system in converting the input fuel to electric energy used by the building. The "Heating Efficiency" is the fraction of heat delivered to the building compared to the total energy input to the system. The heating efficiency therefore represents the efficiency of the system in converting input energy to heat used by the building. The "Delivered Energy Efficiency" is the sum of the delivered electrical efficiency and the heating efficiency, and therefore indicates the efficiency of the system in converting energy from natural gas to both heat and power for the building.

The "Delivered Exergy Efficiency" is an efficiency calculation based on the exergy of the power and heat supplied to the building compared to the exergy of the natural gas fuel input. Exergy differs from energy as exergy is a measure of the quality of the energy, where electrical energy has a relative exergy value (called energy grade function) of 1 as the energy is the highest possible quality (with many uses), while hot water (66°C) has a relative exergy value of 0.00921 as the thermal energy present in this water is of very low quality with few uses (Rosen, et al., 2005). The exergy efficiency therefore lowers the importance of producing hot water and heat as the exergy of these products is much lower than that of electricity. The "Delivered E3 Efficiency" is an alternative efficiency measurement and is commonly used by the co-generation industry, the US Environmental Protection Agency and the Canadian Industrial Energy End-use Data and Analysis Centre (Nyboer, et al., 2014). With this method, it is assumed that 80% of the heat produced could have theoretically been used to produce electricity and thus is subtracted from the total fuel input. Both the exergy efficiency and E3 efficiency are useful metrics that allow for a meaningful comparison of co-generation and tri-generation systems that co-produce different combinations of energy products of different qualities. The equations used for the delivered energy efficiency, exergy efficiency and E3 efficiency are provided in Table 3.1.

Table 3.1. Equations for Delivered Energy, Exergy and E3 Efficiencies

Efficiency	Calculation
Delivered Energy Efficiency (%)	$\frac{Delivered\ Power + Heat\ Delivered + Hot\ Water\ Delivered}{HHV\ of\ Fuel\ Input}$
Delivered Exergy Efficiency (%)[1]	$\frac{Delivered\ Power + 0.00596 * Heat\ Delivered + 0.00921 * Hot\ Water}{0.913 * HHV\ of\ Fuel\ Input}$
Delivered E3 Efficiency (%)[2]	$\frac{Delivered\ Power}{HHV\ of\ fuel - \frac{Delivered\ Heat}{0.8}}$

[1] (Rosen, et al., 2005)
[2] (Nyboer, et al., 2014)

The “Total Efficiency” calculations are similar to the “Delivered Efficiency” calculations; however the total efficiencies considers all heat and power produced by the system, rather than solely the heat and power used by the building. The total efficiencies therefore assess the efficiency of the system in converting natural gas to the total amount of power or heat (or the sum of both) produced. The total efficiencies will therefore always be greater than or equal to the delivered efficiencies as the total efficiencies take into account the heat and power produced that was not used by the building.

3.3.6. CO_2 Emissions

The final section of the GUI provides the metrics to assess the environmental impact of the system and compare it to using the centralized grid and a high-efficiency furnace. The “Direct CO_2 Emissions” provide the CO_2 emissions directly associated with the operation of the SOFC/CAES system. These emissions are due to the combustion of natural gas in the SOFC, and are based on the rigorous Aspen Plus model discussed in Chapter 2. The “Indirect CO_2 Emissions” are the emissions associated with the power purchased from the centralized grid (assumed NGCC at 469 gCO_2/kWh (Energy Information Administration (EIA), 2012)) during times of power underproduction, and the heat produced by a high-efficiency furnace (assumed 290 gCO_2/kWh (Energy Information Administration (EIA), 2012)) during times of heat underproduction.

The “Avoided CO_2” button computes the difference between the emissions of the SOFC/CAES system and the emissions of an NGCC/furnace system if it were used to produce all the power and heat for the building, as indicated in Equation 3. A positive number indicates that the total CO_2 emissions of the SOFC/CAES system (including both direct and indirect emissions) are lower than the emissions associated with the building if all of its power was provided with an NGCC and all of its heat was provided with a high-efficiency furnace.

$$Avoided\ CO_2 = (Emissions\ from\ NGCC + Emissions\ from\ furnace) - (Indirect + Direct\ Emissions\ from\ SOFC\ and\ CAES\ system) \quad (3)$$

The "Percent Reduction" button computes the fraction of avoided CO_2 emissions compared to the total emissions of an NGCC/furnace system, as seen in Equation 4. A large (greater than 20%) percent reduction indicates that implementing the user-defined SOFC/CAES system would drastically lower the CO_2 emissions associated with the building compared to if the building was powered and heated using the current state-of-the-art technologies.

$$Percent\ Reduction = \frac{Avoided\ CO_2}{Emissions\ from\ NGCC + Emissions\ from\ furnace} * 100\% \quad (4)$$

3.4. Conclusions

This chapter discussed the load-following algorithm used to assess the technical feasibility of the proposed SOFC/CAES system. The chapter also discussed a generic graphical user interface analysis tool, programmed in Python, that allows any user to import their specific demand and renewable supply datasets, input their proposed SOFC/CAES performance properties, and then analyses the technical feasibility of their proposed system. The GUI provides extensive information on the ability of the system to follow the provided heat and power demand profiles, a variety of efficiency calculations, and determines the environmental impact of the system and compares it to the current state-of-the-art technologies. The GUI is a tool that streamlines information to the user, and provides a means to assess the ability of the SOFC/CAES system proposed in this work to be analyzed with a wide variety of operating conditions and datasets.

Chapter 4

TECHINCAL ANALYSIS OF SOFC/CAES DISTRIBUTED GENERATION

4.1. Introduction

The previous chapters outlined the models used to determine the outputs of the SOFC/CAES system under various operating conditions, as well as the implementation of these models in a general GUI analysis tool to evaluate the load-following performance of such a system. In this chapter, the GUI tool is used to analyze the performance of the SOFC/CAES system in meeting the heat and power demand of a building located on the campus of McMaster University, Hamilton, Canada.

In 2013, a referendum was passed supporting the development of the Engineering Centre for Experiential Learning (ExCEL) building at McMaster University. One of the initial goals of the building was to implement sustainability technologies to potentially achieve independence from the power grid. The SOFC/CAES system proposed in this work has the potential to help achieve grid-independence, and thus the specific case study to be analyzed in this work was chosen to be the ExCEL building.

4.2. Data Collection and Validation

4.2.1. Heat and Power Data

Since the ExCEL building has not yet been constructed, the hour-by-hour demand profiles are unknown. Instead, the hourly energy demand profile of the John Hodgins Engineering (JHE) building, which is immediately adjacent to the ExCEL building site and serves a similar function (offices, workspaces and laboratories for engineering education), was used instead. The data were provided by Facility Services at McMaster University, which collects hourly energy demand data for every building on campus routinely. The data were scaled down to an average total energy demand of 50 kW, as the ExCEL building is to be significantly smaller than JHE, based on the relative square footage of the two buildings. Historical data for a year, beginning in March 2013, was used for this study.

Unfortunately, the historical data recorded by Facility Services is the sum of heat and power demands, and thus the relative proportion of heat and power had to be estimated. To do this, the hourly heating demand profile was estimated based on and heating degree hours (HDH), using a method provided by Duquette (Duquette, et al., 2014). HDHs represent the relative hourly outdoor temperature to a reference temperature (16°C for this study) in an attempt to quantify the amount of heat needed at a given hour. HDH data for the city of Hamilton was acquired from Environment Canada (Environment Canada, 2014) and used to compute the heat demand profile of the building based on the energy profile provided by McMaster University. It is not expected that the heat demand at a given time will be more than 75% of the total energy demand; therefore any hourly heat demand computed by the Duquette method above 75% of the total energy demand was instead fixed at 75% of the total energy demand at any given hour. The electricity demand profile was assumed to be the remainder of the energy demand of the building not associated with heat demand. The heuristic used to determine the hourly heat and electricity demand profiles is provided in Figure 4.1.

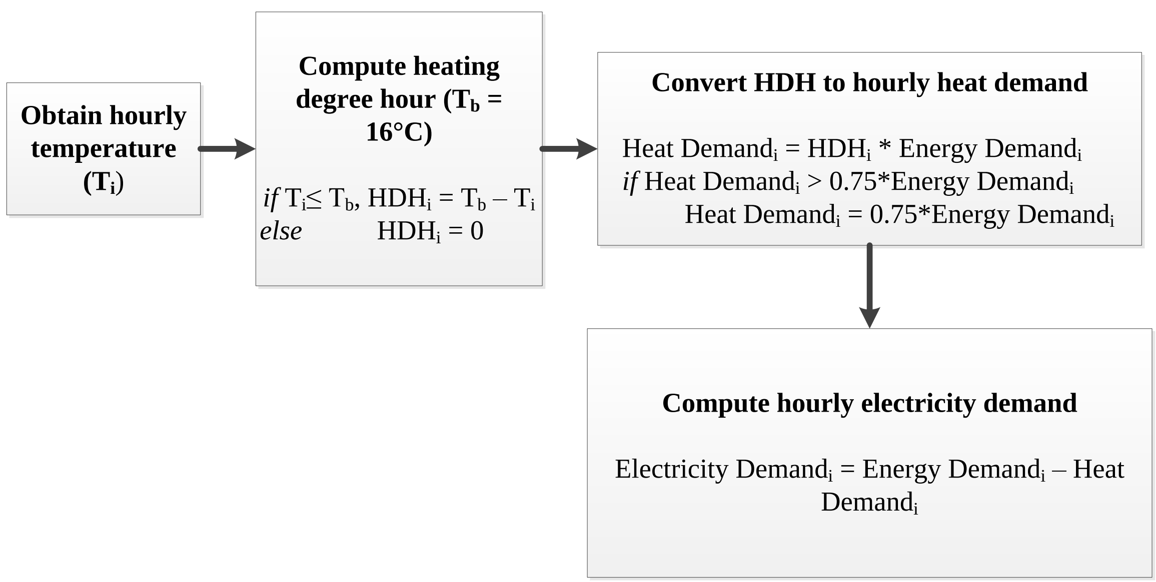

Figure 4.1. Heuristic used to determine hourly heat and electricity profiles based on total energy demand profile.

4.2.2. Renewable Power Supply Data

One of the original design decisions of the ExCEL building was the use of a solar panel array to provide a portion of the power; therefore the proposed SOFC/CAES system was analyzed in combination with a solar panel array with a maximum power output of 50kW. No data exists for the power output of such an array located on McMaster University; therefore the theoretical output of the array was estimated using the RENES renewable energy estimator computer program (Panagopoulos, et al., 2012). The RENES system uses a 54 hour local weather forecast in conjunction with user defined properties of the solar array to compute the estimated hourly power output of the array. A data collection program was developed in Python to obtain the predicted solar panel output over the course of 2 years, from March 2013 to March 2015. This data was then imported to the GUI, discussed in Chapter 3, as the additional renewable supply.

4.3. Implementation of the SOFC/CAES System

As previously mentioned, the case study of interest was the implementation of the SOFC/CAES system for the ExCEL building on the campus of McMaster University. The aim of this work, and one of the original design goals of the building, is to obtain a CHP system capable of producing the majority of heat, hot water and power demanded by the building with a minimal environmental impact. As mentioned in Chapter 2, the majority of the power for the building is provided by the SOFC, with load-following capabilities provided with the integration of the CAES system. The hot water for the building is supplied by some of the waste heat produced by the SOFC. The heat demand is provided by recovering the remaining waste heat produced by the SOFC through an in-floor radiant heating system. The integration of all the SOFC/CAES systems, as well as the solar panel array of the ExCEL building, is depicted in Figure 4.2.

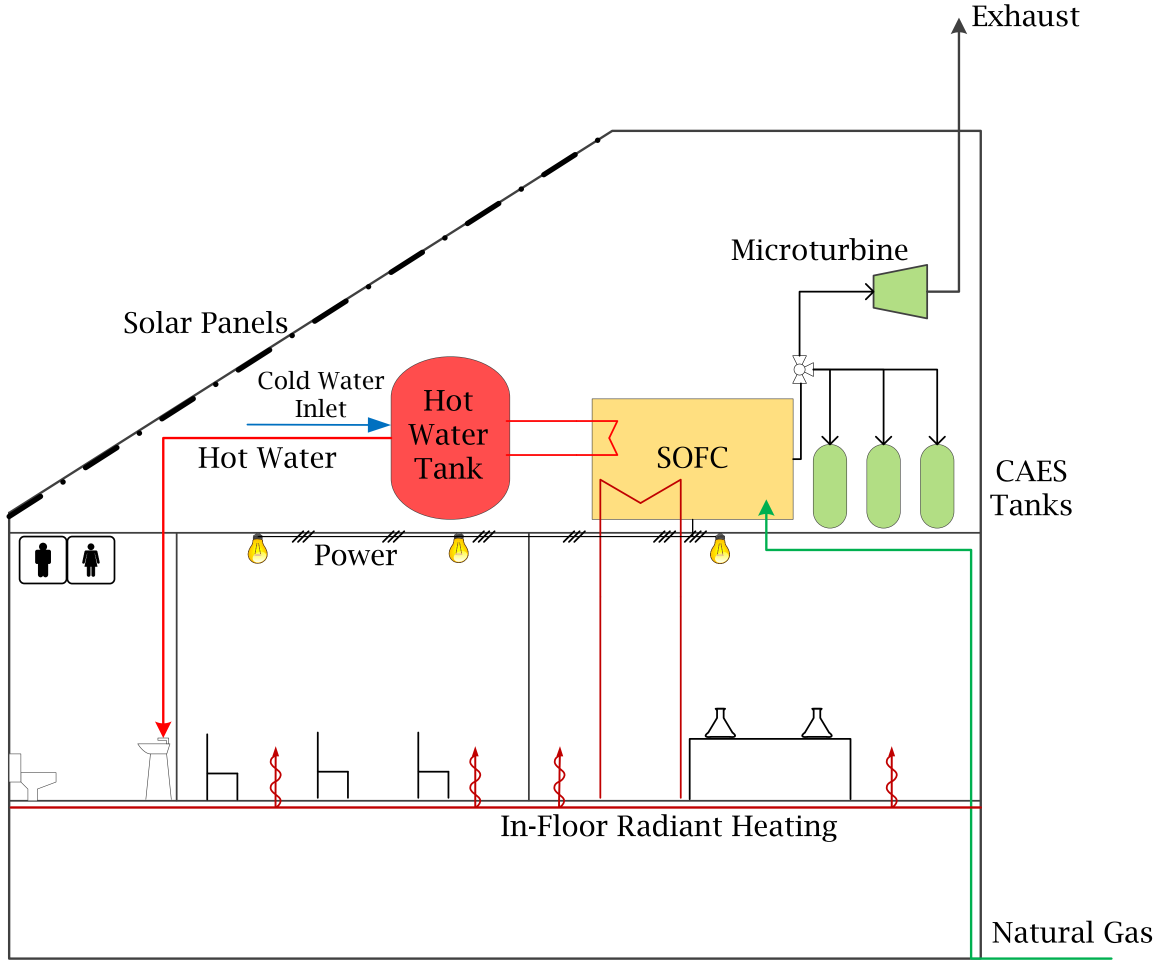

Figure 4.2. Integration of all sub-systems, as well as solar panels, in the SOFC/CAES system

4.3.1. Case studies

Three different SOFC/CAES system configurations were studied to determine load-following performance characteristics of the proposed system. All configurations involved base-load SOFC and CAES operation outlined in Table 4.1; however each case study investigated different FUs of the SOFC unit. The FU of a SOFC is defined as the percentage of fuel that is consumed within the SOFC in order to produce electrical power; therefore a higher FU system will more efficiently produce power since more fuel is consumed in the SOFC, which has a higher efficiency than the downstream combustor. When an SOFC is operated with a lower FU, the thermal-to-electric ratio (TER) increases, meaning the amount of heat produced is significantly increased compared to the amount of electric power produced. A high TER is most suitable for colder seasons (certain portions of winter and fall in Canada, for example), as the heat demand for these seasons is high due to the colder temperatures, and the power demand is low due to a lack of air conditioning. Conversely, a high FU for the SOFC results in a low TER, which corresponds with the high electricity and low heating demand trends seen in hotter seasons, namely spring and summer. The first two case studies involve using a constant FU throughout the whole year: the first case uses a FU of 80%, while the second case uses a FU of 65%. It is worth nothing that the degradation of the cells over time was not investigated in the current study for simplicity. Some studies have indicated FU may affect degradation rates (Hernandez-Pacheco, et al., 2004), although the magnitude of the impact is unknown.

Table 4.1. SOFC/CAES System Assumptions and Conditions

Parameter	Value
Power Producers	
Base-Load SOFC Stack Power (kW)	42.5
Maximum Solar Panel Power (kW)	50.0
CAES Properties	
Minimum Pressure (bar)	15
Maximum Storage (bar)	45
Storage Temperature (°C)	80
Vessel Size (m^3)	50
Compressor Efficiency (%)	75
Turbine Efficiency (%)	75
Additional Properties	
Degradation Rate (%/1000 hrs)	0
DC/AC Inversion Efficiency (%)	95

The third case study investigates the feasibility of a modifiable seasonal fuel utilization (MSFU) system, where the SOFC FU is 80% for spring and summer, and then the FU is modified to 65% for autumn and winter. The FU of the SOFC is primarily dictated by the electrochemical properties, fuel distribution, and transport phenomena of the anode (Fang, et al., 2015). It is difficult to modify the electrochemical properties of the anode; therefore the FU for the MSFU case is modified by varying the natural gas feed rate and humidity. A higher natural gas feed rate results in less residence time for the fuel in the SOFC, thereby lowering the FU (Hernandez-Pacheco, et al., 2004), while a higher humidity also reduces the FU by lowering the oxidation potential of the fuel. When the FU is modified from 80% to 65%, the natural gas feed flow is increased in order to maintain the base-load SOFC output at a constant 42.5 kW. The FU of the SOFC is modified due to the differences in heat and electricity demand trends throughout the year, and the synergy that these differences have with different FU performance characteristics. Although frequent changes to the operating conditions might cause operability difficulties, it is reasonable to transition the stack from one steady state to another in a controlled and planned manner only once every six months or so. Although SOFC steady state transitioning is an area of active research, preliminary studies have shown that simple fuel transitions for some systems can safely be achieved in about one to two hours (Harun, et al., 2014). Therefore, for the sake of simplicity, it is assumed that the fuel utilization transition for the proposed system can be accomplished in less than an hour. The costs and impacts of this transition are neglected. For the purposes of the study, the dates at which the fuel utilizations were fixed as shown in Figure 4.3, which provides the daily average heat and power demand over the course of the year. These FU transition dates were somewhat arbitrarily chosen to coincide with the calendar dates for the beginning of spring and autumn. In practice, the dates should be selected in advance based on some guess at when it is most optimal to do so.

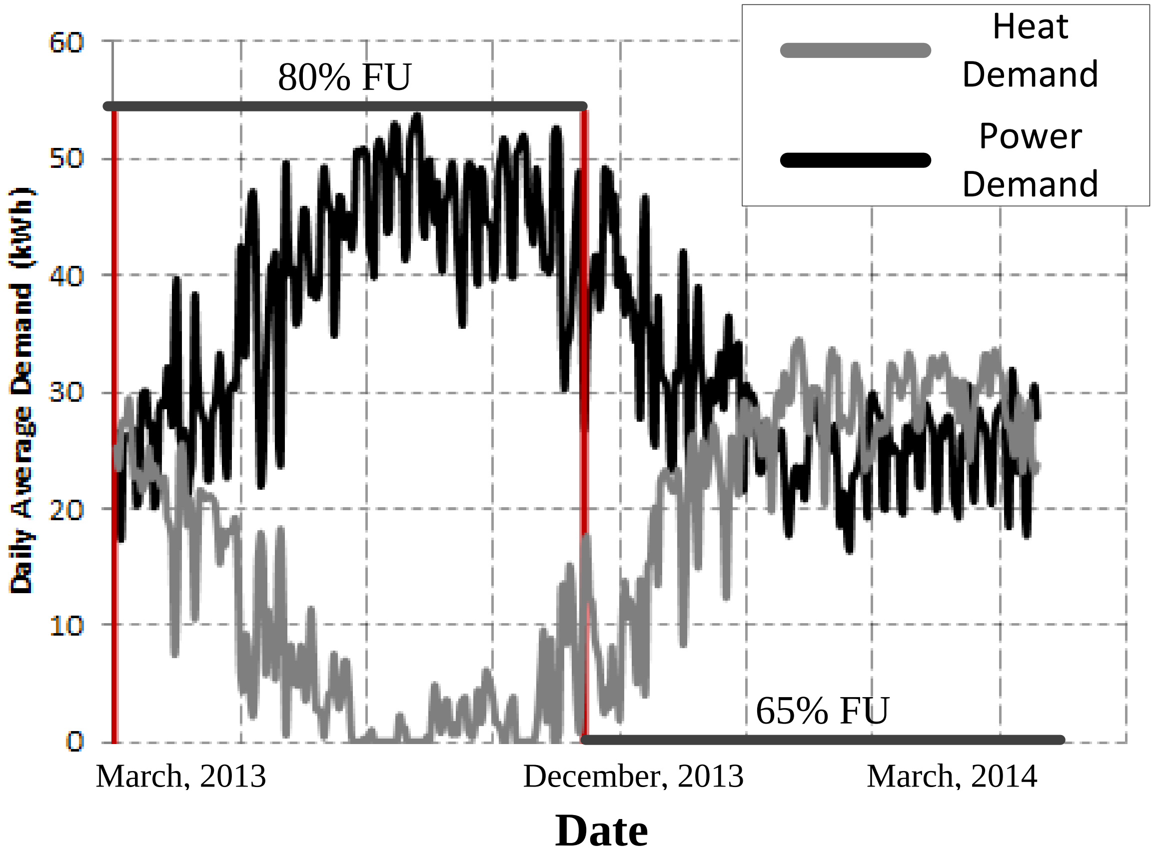

Figure 4.3. Daily average power and heat demand from March 21st, 2013 to March 20th, 2014

4.4. Results and discussion

4.4.1. Load-following properties

The overall load-following properties of the three case studies are outlined in Figure 4.4. It can be seen that the proposed system, in all case studies, is able to provide more than 89% of all electricity demand and more than 57% of all heat and hot water demand. As expected, the 80% FU system was able to meet the most electricity demand while meeting the least of the heating demand due to the higher amount of energy contained in the fuel being converted to electrical energy in the fuel cell itself, as opposed to thermal energy generated in the post-combustion system. The 65% FU system was found to meet the least amount of electricity demand while meeting the most heating demand for the opposite reasons. Interestingly, the MSFU system demonstrated the synergy that could be captured by using different SOFC FUs in different seasons, providing more than 92% of the electricity demand and simultaneously providing more than 71% of the heat and hot water demand. These results indicate that there are trade-offs between the heat and load-following capabilities, which are particularly when examining seasonal trends.

It should be noted that many decisions were made in the design of this system, such as CAES storage temperature, hydronic floor heating operating temperatures, and heat exchanger sizing. Varying these design parameters will affect the quantitative results; however the qualitative results, such as the 80% FU system providing the most power and the 65% FU system providing the most heat, will not be affected. Changing these parameters will affect all the case studies in a similar, although not equal, way resulting in consistent qualitative results.

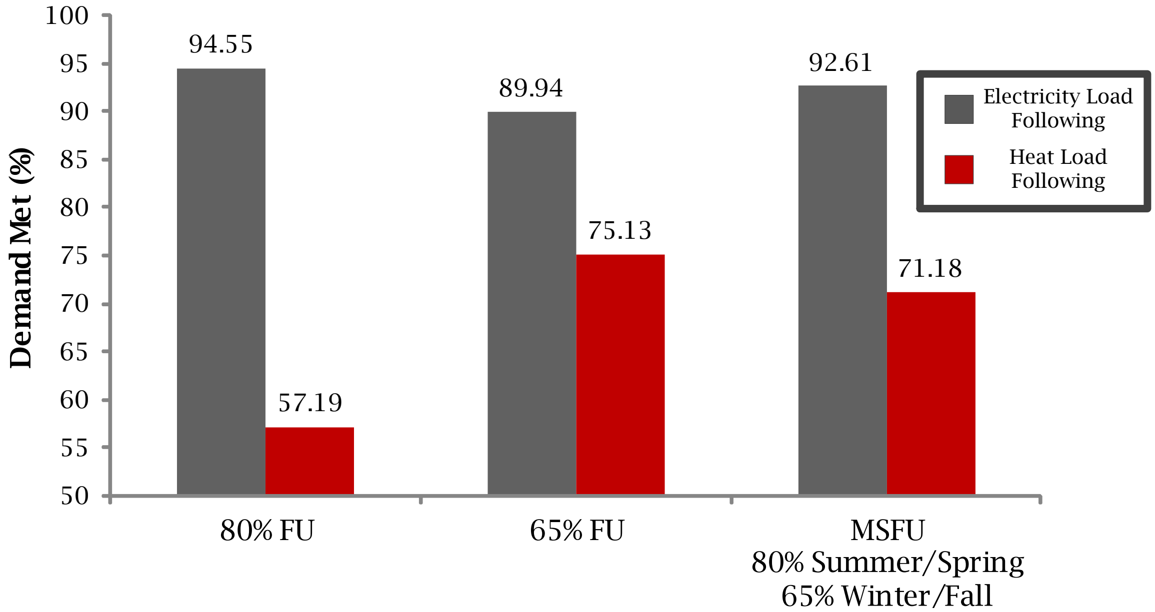

Figure 4.4. Load-following properties of the three case studies for the SOFC/CAES DG system

An example week from the summer and winter load-following profiles, for both the heat and electricity demands of the 80% FU case and the 65% FU case, are provided in Figure 4.5 and Figure 4.6, respectively. It can be seen in the figures that the summer heating demand is relatively low and the power demand is relatively high. During this season, the 80% FU case is able to meet all of the heat demanded by the building, while simultaneously meeting more of the electricity demanded when compared to the 65% FU case study. The underproduction of power occurs since the storage vessel becomes depleted of all stored energy during periods of relatively high demand, thus the CAES is unable to contribute to the power production of the system and provided power is simply limited to the power produced by the base-load SOFC and the on-site solar panels. The 80% case study is able to provide more power compared to the 65% case due to the lower

TER of the 80% system; since less heat is produced, the 80% FU case requires significantly less air cooling in order to avoid heat overproduction, resulting in significantly less parasitic power loads and therefore higher net power production. Overall the 80% FU system is superior at matching both heat and electricity demands during the summer months when compared to the 65% FU system.

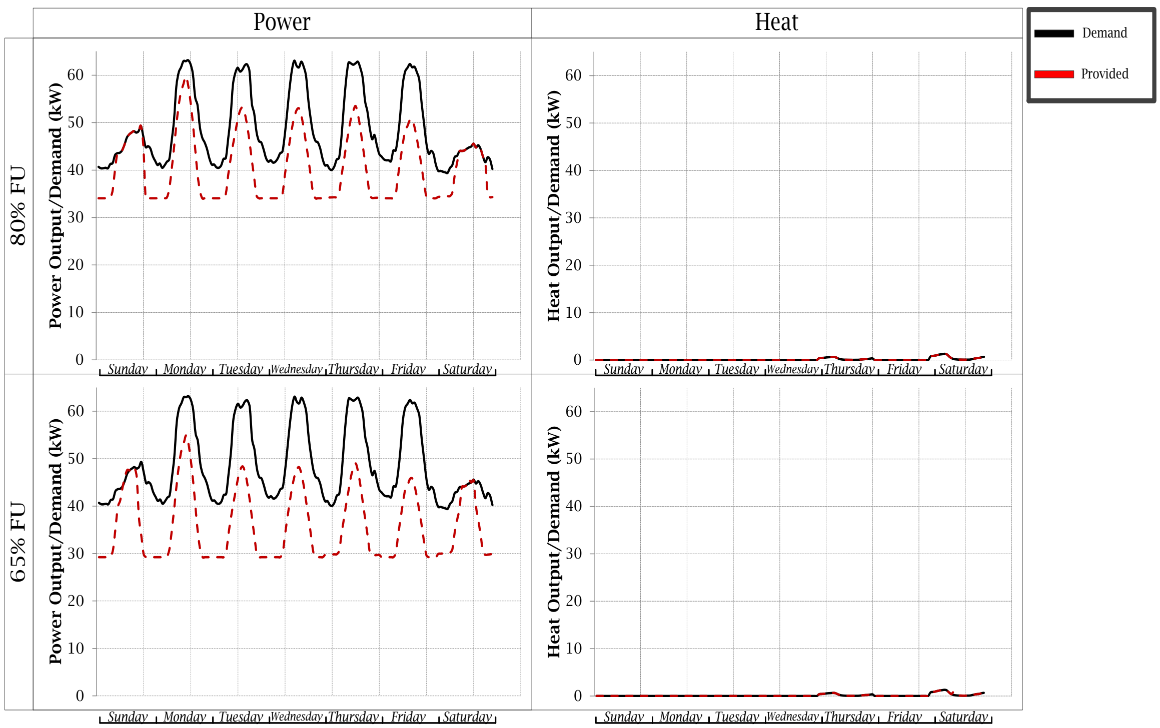

Figure 4.5. A week (June 23rd, 2013 to June 29th, 2013) of the summer load-following profiles for power and heat demand

In contrast, the example winter week had relatively higher heat demand (due to the colder temperatures) and low power demand (due to the absence of air conditioning units used to regulate building temperature during the summer). In fact, during the winter months it was observed that the base-load output of the SOFC combined with the availability of solar energy was usually enough to meet even the highest peak power demand. This resulted in a reduced effectiveness of the CAES system because the storage capacity is not large enough to store most of the overproduction, and demand rarely exceeded the base-load supply, making CAES discharges a rarity. Consequently, the 65% FU system outperforms the 80% FU system since it meets more of the heat demand with lower power overproduction due to its lower TER. The 65% system is thus overall more efficient in the colder seasons as the consumed fuel is directed to producing more useable forms of energy (thermal), rather than producing even more excess power as similar to the 80% FU system.

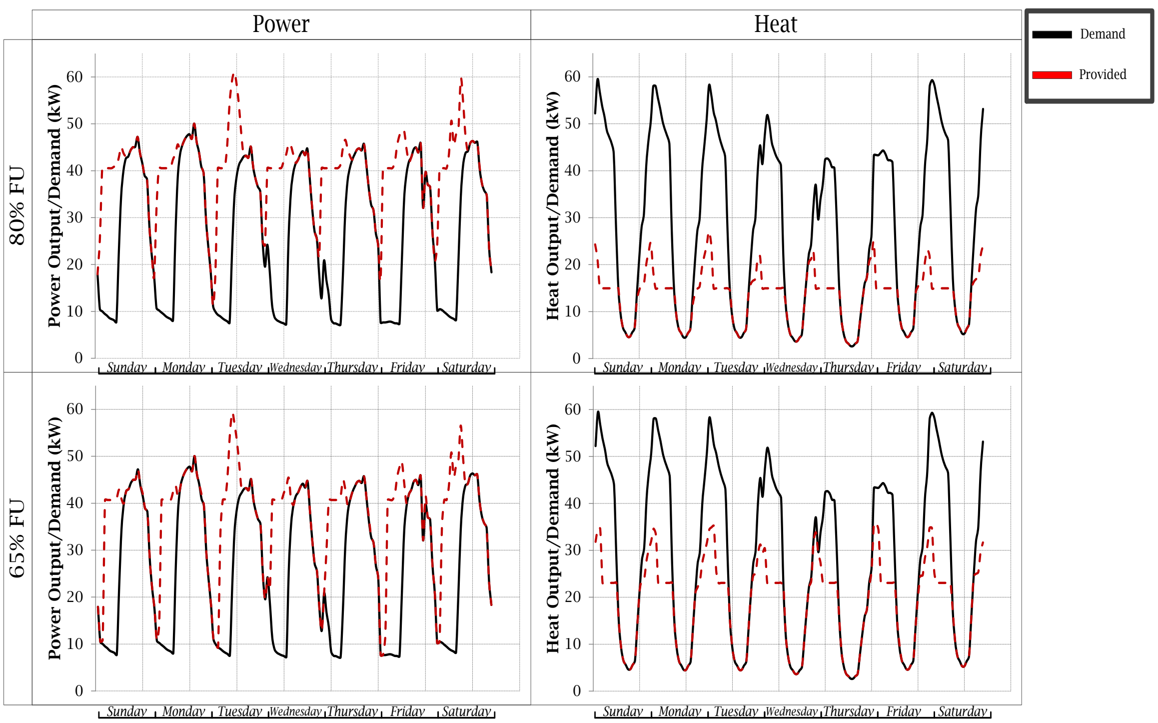

Figure 4.6. A week (December 22nd, 2013 to December 28th, 2013) of the winter load-following profiles for power and heat demand

These results correspond well with the theoretical practicality of the MSFU system, as the 80% FU system outperforms the 65% FU system during periods with higher electricity demand relative to thermal demand (summer months), while the 65% FU system is superior during colder periods with low electricity demand. The MSFU system provides an improved load-following strategy as the system has the superior summer load-following trajectory of the 80% FU system seen in Figure 4.5, while having the superior winter load-following trajectory of the 65% FU system seen in Figure 4.6, resulting in the best combination of heat and power load-following capabilities, seen in Figure 4.4.

4.4.2. Overall annual system performance

The performance results for the system at each FU investigated throughout the course of one year of operation are presented in Table 4.2. The 80% FU system has the highest total system thermal efficiency (by higher heating value, HHV) due to the fact that the 80% FU system does not produce a significant amount of unused waste heat that must be air cooled. Also, an SOFC operating with an 80% FU will inherently have a higher electrical efficiency than a 65% FU SOFC due to the fact that the 65% FU system requires more natural gas feed in order to maintain the 42.5 kW SOFC output. The 65% FU system also produces more heat than the other two cases, which results in a significant amount of air cooling during the summer months, resulting in a lower efficiency. The 65% FU system thus has a drastically lower total thermal efficiency (42.0 %HHV) when compared to the 80% FU case (57.1 %HHV). The MSFU case provides an effective hybridization of the two other case studies in that it provides a significant amount of power with a reasonably high efficiency of 50.6 %HHV (6.5 percentage points less than the 80% FU case and 8.6 percentage points more than the 65% FU case) while also providing a significant amount of heat with minimal air cooling.

It should be noted that although an air conditioning unit is chosen as the method for cooling the exhaust during periods of low heat demand in this study, it is not the sole solution. Another option is the use of an absorption cooler, which uses heat, rather than electricity, as an energy source to drive the cooling of a heat engine. The excess heat from the SOFC exhaust could theoretically be used as the heat source for absorption cooling in the hotter summer and spring months and would likely increase the overall efficiency of the system; however this alternative was not explored as absorption cooling requires significant infrastructure and would be impractical for a building the size of the one explored in this study (Wang, et al., 2013). The absorption cooler alternative is therefore more practical for larger commercial buildings or communities with cooling demands exceeding 200 kW (Wang, et al., 2013) and is not investigated in this study.

Table 4.2. Overall System Performance Metrics

	Case Study		
Parameter	**80% FU**	**65% FU**	**MSFU**
Efficiencies			
Total Efficiency	57.1 %HHV 63.3 %LHV	42.0 %HHV 46.5 %LHV	50.6 %HHV 56.1 %LHV
Total Delivered Efficiency	46.5 %HHV 51.6 %LHV	35.6 %HHV 39.5% LHV	41.8 %HHV 46.3 %LHV
Electrical			
Total Power Delivered to Building (kWh)	233,360	219,601	232,375
Total Overproduction (kWh)	84,481	70,810	76,877
Total Power Purchased from Grid (kWh)	16,258	30,017	18,245
Heating			
Total Heat Produced by SOFC/CAES system (kWh)	102,428	159,333	132,031
Total Air Cooling (kWh)	21,038	52,355	30,732
Emissions			
Direct CO_2 Emissions (tonne/year)	158.89	192.23	175.28
Indirect CO_2 Emissions Associated with Grid Power (tonne/year)	6.51	13.41	7.29
Indirect CO_2 Emissions Associated with Furnace Heat (tonne/year)	18.76	10.92	13.17
Total CO_2 Emissions (tonne/year)	184.16	216.56	195.74
CO_2 Reduction Compared to status quo (NGCC + furnace) (%)	26.95	8.70	19.98

Due to the higher overall efficiency of the 80% FU system, this case study also has the lowest total (sum of direct and indirect) CO_2 emissions (184.16 tonnes CO_2/year), and therefore the highest amount of CO_2 reduction compared to a state-of-the-art system that uses a centralized NGCC plant to provide all of the power, and an on-site, high efficiency furnace to provide all of the heat. The 80% FU system, however, does not have the least amount of indirect CO_2 emissions due to its low heat production, thereby requiring a larger furnace and resulting in more emissions not directly associated with the SOFC/CAES system. The 65% FU system, with its low efficiency power production, has the highest total CO_2 emissions (216.6 tonnes per year) due to its large amount of direct emissions. Once again, the MSFU system rests in-between the other cases, with a moderate amount of direct emissions (175.3 tonnes of CO_2 per year) and the lowest amount of indirect emissions (20.5 tonnes CO_2 per year). The MSFU case also has very limited CO_2 emission increase compared to the 80% FU case (6.97 percentage points); however the MSFU system provides significantly improved heat load-following capabilities and reduces overall system overproduction. Overall, the combined SOFC/CAES system in conjunction with the on-site solar panels, in all case studies, shows improvement in terms of global CO_2 emissions when compared to the current state-of-the-art energy producing technologies considered as the alternatives in this work.

4.5. Sensitivity Analyses

4.5.1. Effect of SOFC Size

The performance of the SOFC/CAES system is highly dependent on the base-load power output of the SOFC; therefore the size of the SOFC was varied to determine its effect on the applicability of the system for the McMaster dataset. The base-load power of the SOFC, with a FU of 80%, was varied between 29.75 kW (70% of the base case) and 55.25 kW (130% of the base case) while keeping all other variables constant. The changes in some of the performance metrics are seen in Figure 4.7. The amount of electricity purchased from the grid is by far the most sensitive variable as a smaller SOFC will be unable to meet the majority of the peaks seen in the highly demanding summer months. Interestingly, the total thermal efficiency is consistent between all SOFC sizes, varying between ±0.65% (0.5 percentage points) of the base case efficiency. The increased fuel consumption from the larger SOFC results in a moderate increase in CO_2 emissions; however the lack of storage for this increase in power results in a significant portion of the power to be wasted and does not drastically improve the load-following capabilities of the building.

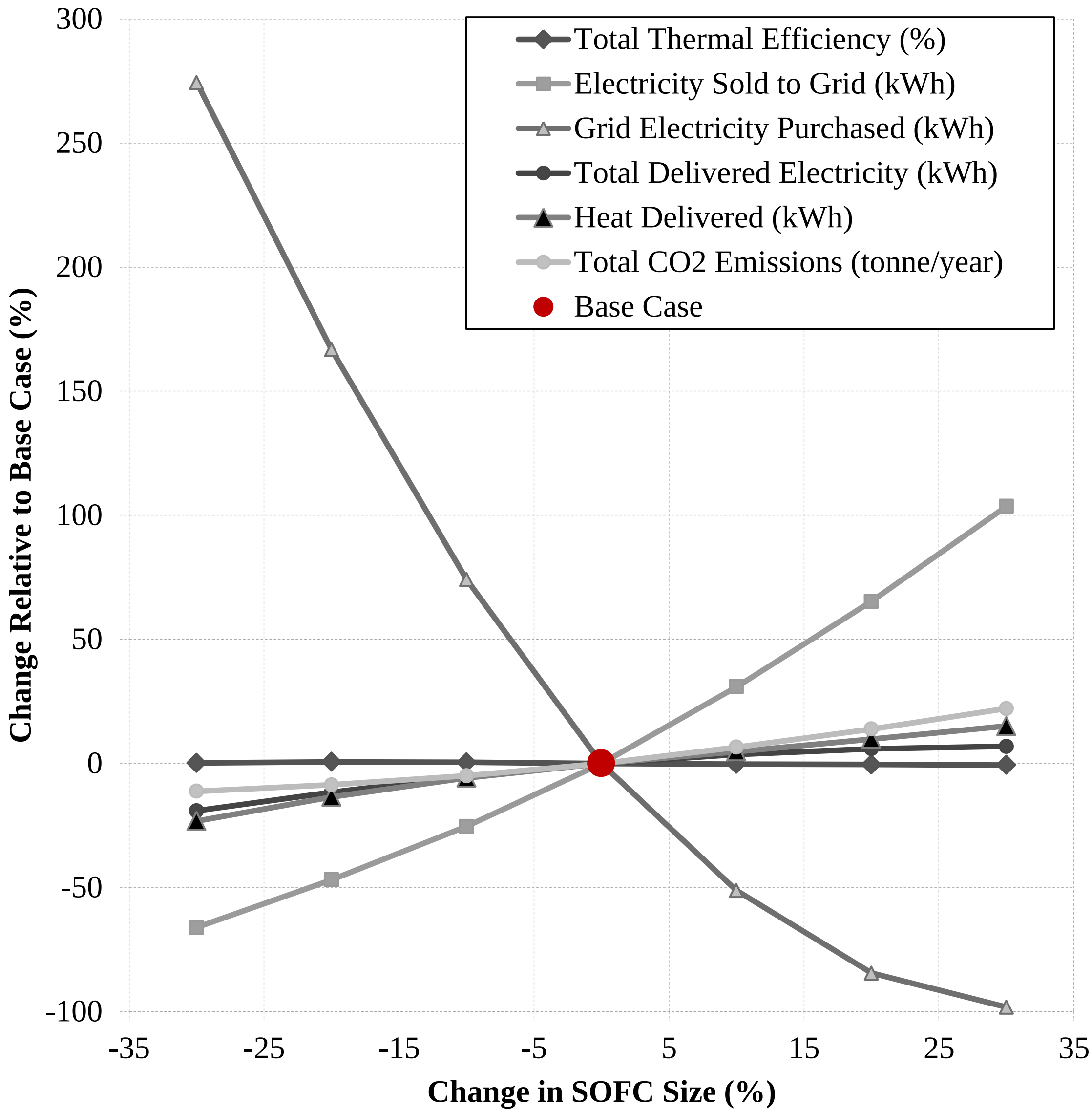

Figure 4.7. Effect of SOFC size on system performance

4.5.2. Effect of CAES Size

Another important factor in the performance of the proposed system is the maximum storage capabilities of the CAES vessel. The maximum storage energy of the CAES was varied from 120 kWh (80% of base case) to 240 kWh (160% of base case), with all other variables at their base values from the 80% FU case in Section 4.3. The sensitivies of the major load-following metrics to variations in the CAES vessel size are depicted in Figure 4.8.

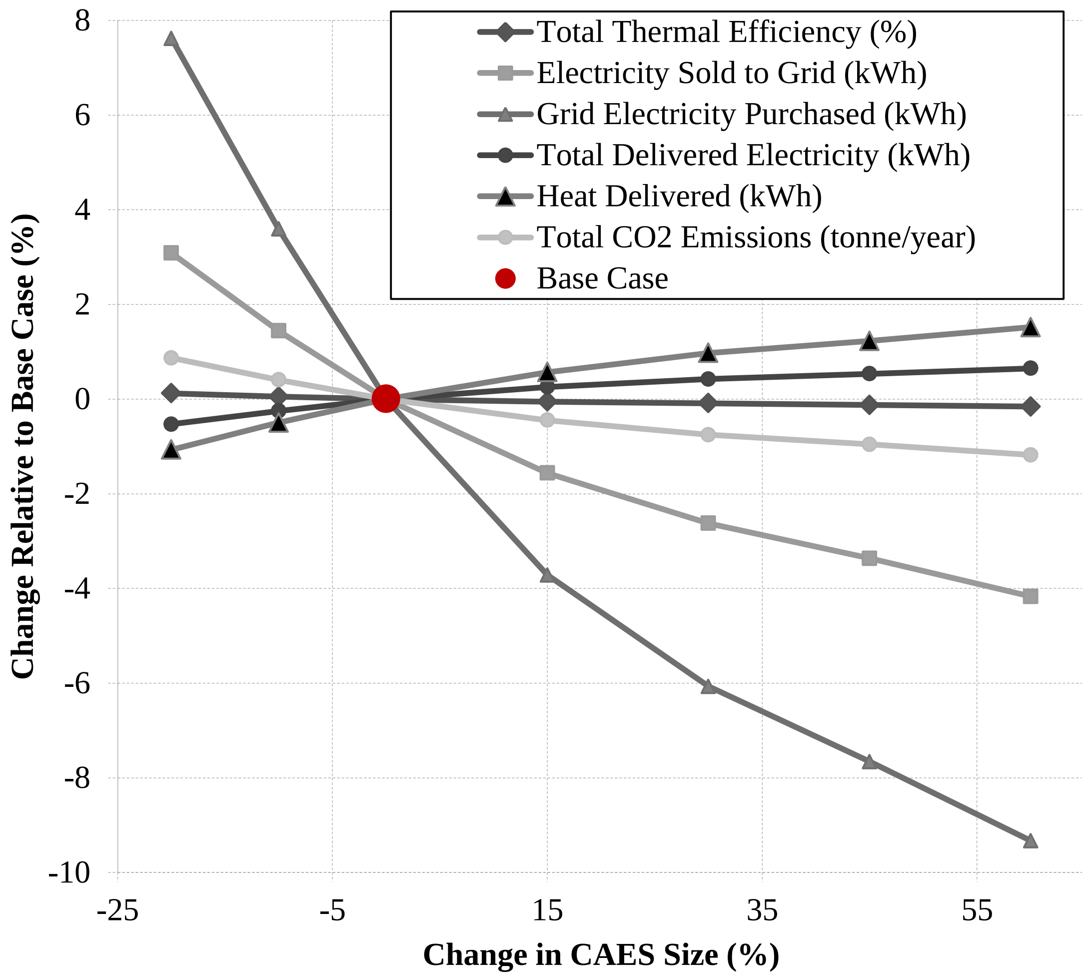

Figure 4.8. Effect of maximum energy storage on system performance

It should be noted that the scale of the changes seen in varying the CAES size are, at times, a tenth or less of the changes associated with varying SOFC size; thereby indicating that the CAES size has a significantly lesser impact on the performance of the system. The main impact of the CAES is on the overall grid-independence of the system as increasing storage capabilities has the biggest impact on the electricity sold to the grid and the electricity purchased from the grid. The thermal efficiency is, as with the SOFC size, nearly unaffected by the CAES changes as the total amount of power does not vary by a significant margin. An interesting trend is that the amount of heat provided by the system increases slightly with CAES size, indicating that the ability to integrate the CAES charging cooling requirements with the heating system does provide a significant amount of heat for the building.

4.6. Conclusions

This chapter examined the technical feasibility of an integrated SOFC/CAES system for the distributed generation of heat, hot water, and power for a new building on the campus of McMaster University. It was found that such a system was able to efficiently provide the vast majority of power demanded, while also meeting the majority of heat demand. Three case studies were investigated to determine the effect of the SOFC FU on overall system performance, as well as seasonal system performance. The MSFU case where the fuel utilization was changed twice per year, such that the FU was high in the summer months (periods of low heat demand and high electricity demand) and low in the winter months (vice-versa), resulted in the best overall load-following performance, with a 19.98% reduction in CO_2 emissions compared to if the power and heat for the building were provided by a NGCC and high efficiency furnace, respectively. The SOFC size was found to dramatically affect the amount of electricity purchased from or sold to the grid, while having a moderate impact on heat provision and CO_2 emissions. The CAES storage capabilities mainly affected the ability of the system to operate without reliance on the grid, with a larger CAES vessel resulting in a drastic decrease in electricity transfer with the grid; however the impact of the CAES size is significantly less than that of the SOFC size.

Chapter 5

ECONOMIC ANALYSIS OF SOFC/CAES DISTRIBUTED GENERATION

5.1. Introduction

The previous chapter demonstrated the technical feasibility of the proposed SOFC/CAES system for load-follow distributed generation, using a case study of the ExCEL building located on the campus of McMaster University. The system is able to provide the majority of the heat and power demanded by the building while reducing the CO_2 emissions associated with the building when compared to the current state-of-the-art technologies. In this chapter, the economics of the proposed system are assessed, including total annualized cost (TAC) and the cost per kWh of energy provided to the building. The costs of the SOFC/CAES system are compared to other DG technologies, including a diesel generator for power and a high-efficiency furnace for heat, as well as a system that uses a larger SOFC without CAES load-following capabilities.

5.2. Capital Cost Estimation

The capital cost of the water pump (Pump 1 in Figure 2.2) and the CAES vessel were determined using Aspen Capital Cost Estimator v8.0. The cost of the CAES discharge microturbine was determined based on data provided by ICF International (Energy and Environmental Analysis, 2008). The capital cost for the remaining equipment (aside from the SOFC, post combustor and solar panels) was determined from capital cost correlations provided in Seider & Seader (Seider, et al., 2009), with free on board (FOB) cost converted to total direct costs using factors also provided in Seider & Seader. The correlations were used for these pieces of equipment as Aspen Capital Cost Estimator was unable to provide an estimate for them at such a small scale. The correlations inherently have error associated with them; however they provide an appropriate estimate of the cost for this study. The cost of the SOFC was determined based on the findings of the NETL (National Energy Technology Laboratory, 2013), and includes the cost of the post combustor unit. The cost of the solar panel array was estimated from data provided by the Solar Energy Industries Association (Solar Energy Industries Association, 2014). The costs of each piece of equipment, as well as the total capital cost of the system for the 80% FU, 65% FU, and MSFU cases are presented in Table 5.1. All costs were scaled to 2013 prices based on the Chemical Engineering Plant Cost Index.

Table 5.1. Capital Cost Estimates for SOFC/CAES System

	80% FU	**65% FU**	**MSFU**
Unit	**Capital Cost ($)**	**Capital Cost ($)**	**Capital Cost ($)**
Turbines			
CAES Turbine 1	$2,200	$2,200	$2,200
Compressors			
CAES Compressor 1	$47,500	$66,300	$66,300
CAES Compressor 2	$53,100	$46,900	$53,100
Vessels			
CAES Storage Vessel	$191,500	$191,500	$191,500
Blowers			
Air Blower 1	$8,700	$9,300	$9,300
Air Blower 2	$1,200	$2,100	$2,100
Pumps			
Water Pump	$16,900	$16,900	$16,900
Heat Exchangers			
Steam Generation (HX-1)	$3,400	$3,500	$3,500
NG Preheat (HX-2)	$3,700	$3,800	$3,800
Air Preheat (HX-3)	$4,800	$4,800	$4,800
CAES Discharge Preheat (HX-4)	$7,500	$7,500	$7,500
Hot Water Generation (HX-5)	$4,000	$3,500	$4,000
SOFC			
SOFC Stack (Single Stack)	$446,300	$446,300	$446,300
Solar Panels			
Solar Panels	$250,000	$250,000	$250,000
Flash Drums			
CAES Flash	$5,200	$4,800	$5,200
Total	$1,046,000	$1,059,400	$1,066,500

The capital costs of the three cases are extremely similar (1.97% difference between the MSFU and 80% FU cases) due to the fact that the SOFC and solar panels contribute more than 65% of the total capital cost and remain consistent between the three systems.

5.3. Operating Cost Estimation

The operating cost of the SOFC/CAES system exists due to the consumption of natural gas, the purchasing of grid power during certain periods of peak power demand, and the usage of a furnace during certain periods of peak heat demand. When power is purchased from the grid, it is assumed that the price of electricity is at the on-peak price of 14¢/kWh (Horizon Utilities, 2015). It is assumed that the overproduced power that is unable to be stored is sold back to the centralized grid at half the off-peak electricity price of 7.7¢/kWh (Horizon Utilities, 2015). These assumptions are conservative as they represent worst case scenarios for purchasing and selling of electricity. The natural gas consumed by the SOFC is purchased at a price of 20.0¢/scm (Ontario Energy Board, 2015). The heat produced by the furnace is assumed to be produced at a price of 2.95¢/kWh (Natural Resources Canada, 2012). The annual operating costs of the system is the sum of cost of the natural gas consumed, the grid power purchased, and the heat produced, with the credit from the power overproduction being subtracted.

5.4. Total Annualized Cost and Cost of Electricity

The total annualized cost (TAC) of the system was computed for each system. The plant lifetime was assumed to be 20 years, with a new SOFC stack purchased after 10 years. After the 20 year lifetime, it was assumed that 15% of the initial capital, not including either SOFC stack, could be reclaimed from the remaining equipment. The TAC was therefore computed as follows:

$$TAC = \frac{0.85*(Initial\ Capital)+2*SOFC\ Price}{20} + Annual\ Operating\ Cost \qquad (5)$$

The total energy cost was computed in order to assess the cost of producing energy for the systems. The cost of energy was based on the useful energy delivered to the building, rather than the total amount of energy produced, as seen in Equation 6. The cost of electricity (COE) and cost of heat (COH) for each system was also computed in order to provide a comparison to current market prices, as well as other DG systems. The COE and COH calculations are provided in Equation 7 and Equation 8, respectively.

$$Energy\ Cost = \frac{TAC}{Annual\ Power\ Delivered + Annual\ Heat\ Delivered} \qquad (6)$$

$$COE = Energy\ Cost * \frac{Annual\ Power\ Delivered}{Annual\ Power\ Delivered + Annual\ Heat\ Delivered} \qquad (7)$$

$$COH = Energy\ Cost * \frac{Annual\ Heat\ Delivered}{Annual\ Power\ Delivered + Annual\ Heat\ Delivered} \qquad (8)$$

The TAC and COE of the SOFC/CAES case studies were compared to those of two other DG strategies. The first strategy employs a large diesel generator for power production and uses a high-efficiency furnace for heat, while the second strategy uses a larger SOFC, with a base-load power of 70kW, 64.7% larger than the base case (as this is the highest electricity peak for the year), to ensure it is able to meet the highest electricity peak, a high-efficiency furnace for heat, but without a CAES for power production. The comparisons of all the systems are provided in Table 5.2.

Table 5.2. TAC and Electricity Cost Comparison for DG Systems

System	TAC ($/year)	Energy Cost (¢/kWh)	COE (¢/kWh)	COH (¢/kWh)
80% FU	72,105	22.91	16.98	5.92
65% FU	75,556	23.14	15.56	7.58
MSFU	73,551	22.04	15.35	6.69
Generator & Furnace	229,520	59.04	37.43	21.62
Large SOFC & Furnace without CAES	119,530	30.75	19.49	11.26

The 80% FU has the lowest TAC due its lower fuel consumption costs; however its wasteful power overproduction during the winter months and drastic decrease in heat production results in the highest COE of the SOFC//CAES case studies. With the lowest power production and the highest fuel consumption, the 65% FU system has the highest TAC and energy cost of all the SOFC/CAES systems. Interestingly, the improved heat load-following capabilities of the MSFU system does not result in a drastic increase in TAC (only a 2% increase) compared to the 80% FU case, and thus the MSFU system has the lowest energy cost and the lowest COE of all cases.

Table 5.2 also indicates that the costs of all SOFC/CAES systems are lower than the other DG strategies. The high electricity cost of the large SOFC & furnace system is due to the fact that the capital cost associated with purchasing a large SOFC is 65% greater than the SOFC/CAES system; however the large SOFC only delivers 36% more power to the building, compared to the 65% FU case, and only provides 27% more power compared to the 80% FU case. The slight increase in power provision does not off-set the massive increase in capital cost, thereby increasing the COE of the large SOFC system. The diesel generator and furnace combination has, by far, the largest TAC and more than double the COE of all the SOFC/CAES cases. This is due to the fact that a diesel generator is an inefficient method to produce electricity and therefore consumes a significant amount of diesel throughout the course of the year.

Although the SOFC/CAES system is the most cost effective solution of the DG systems investigated, it is 1.35 to 2.98¢/kWh more expensive compared to the current market prices for on-peak, highest price, electricity. It is also 2.97 to 4.93¢/kWh more expensive for heat production compared to current prices for heat generation. It is therefore better, in a purely economic sense, to rely solely on grid power and a high efficiency furnace as this is the cheapest alternative. This, however, is not a characteristic of the SOFC/CAES system, but is a characteristic of DG in general, as a larger centralized system will benefit from a proportionally lower capital cost due to economies-of-scale.

5.5. Sensitivity Analyses

5.5.1. Effect of SOFC Size

As with the technical feasibility, the sensitivity of the cost of electricity to major design choices was investigated. The base-load power of an 80% FU SOFC was once again varied between 23.75 kW and 55.25 kW (±30% of base case) with all other variables held constant and the system electricity cost was analyzed. Increasing the size of the SOFC, and thus decreasing the amount of electricity purchased from the grid, results in an overall decrease in the cost of electricity for the system, as seen in Figure 5.1, until the point where the capital investment associated with purchasing a significantly larger SOFC does not offset the reduction in grid electricity purchases. The cost of avoiding CO_2 emissions, computed as the ratio of TAC to annual avoided CO_2 emissions, drastically increases with SOFC size, indicating significant diminishing returns in the environmental benefits of the system with larger SOFCs. Interestingly, the sensitivity of the cost of independence, computed as the ratio of the total system cost over the lifetime to the power percentage demand met of the system, appears to be parabolic in nature. This indicates that the trade-offs between electricity cost and grid-independence can be minimized, and is nearly minimal at the base-case. For a building attempting to achieve near grid-independence at a reasonable price, the solution where these trade-offs are minimized provides the best solution for the size of the SOFC.

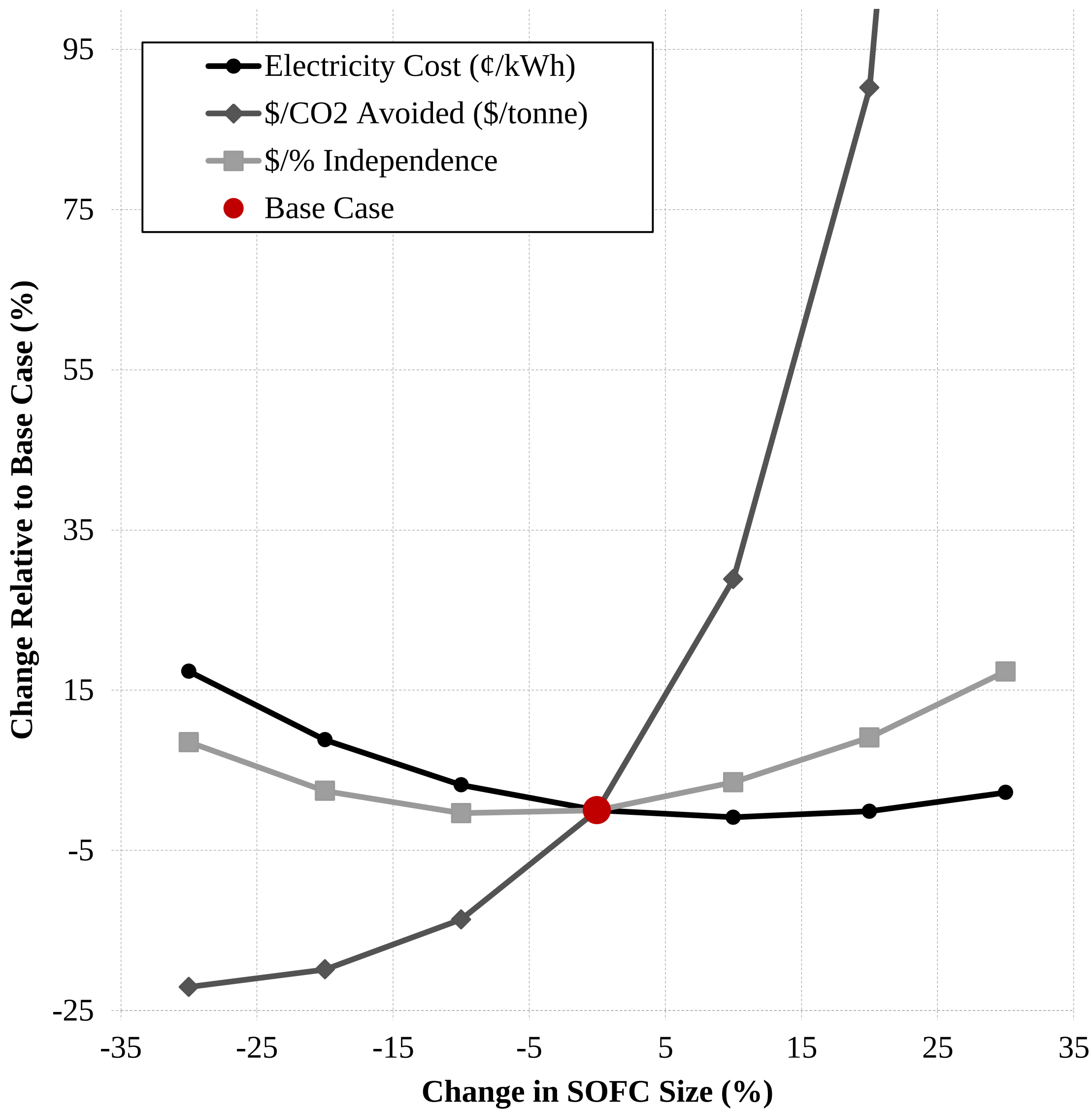

Figure 5.1. Sensitivity of system economics to the size of the SOFC

5.5.2. Effect of CAES Size

The sensitivity of the system electricity cost to the CAES size was also investigated by manipulating the maximum CAES energy storage between 120 kWh (80% of base case) and 240 kWh (160% of base case). The price of electricity increases with CAES maximum storage due to the significant increase in capital investment associated with purchasing a larger CAES storage vessel. The cost per CO_2 avoided is quite sensitive to the size of the CAES vessel as the CAES has a very minimal effect on the emissions (both direct and indirect) associated with the system (as seen in Figure 4.8); therefore the increase in price for a larger CAES vessel does not necessarily result in an equal change in CO_2 emissions. The parabolic nature of the cost per CO_2 avoided indicates that the cost reduction associated with a smaller CAES vessel does not outweigh the emissions benefits of the increased grid-independence. The cost per percentage increase in grid-independence is also parabolic in nature; however is more sensitive on the positive side of the base case. This indicates that there are significant diminishing returns associated with purchasing a larger vessel than the CAES vessel size used in the base case for grid-independence. If grid-independence is desired a larger CAES vessel does provide an increase in independence; however it is no longer beneficial from an economic standpoint.

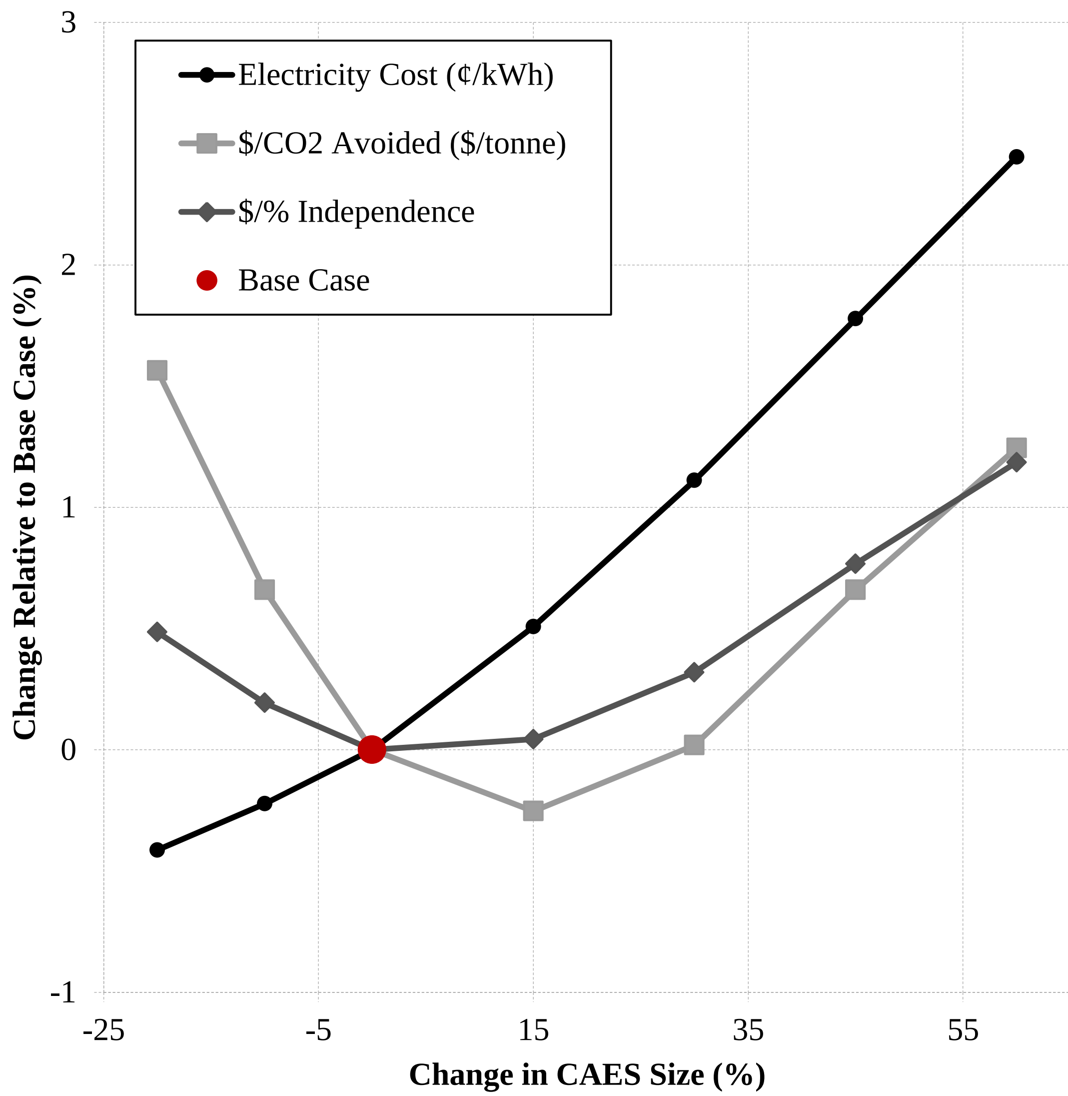

Figure 5.2. Sensitivity of system economics to the size of the CAES system

5.6. Conclusions

This chapter presented the economics associated with implementing the SOFC/CAES system for a building located on McMaster University, and compared it to other DG technologies. It was found that the SOFC/CAES system is the most cost effective of the DG technologies investigated, providing electricity at a maximum cost of 16.98 ¢/kWh. This cost is, however, significantly higher (nearly 150% greater) than the cost of off-peak electricity in Hamilton, and 21% greater than the cost of on-peak electricity. The price of electricity was found to be extremely sensitive to the SOFC base-load power and moderately sensitive to the CAES maximum energy storage. A larger SOFC is cost-beneficial until the SOFC becomes so large it is simply overproducing power for the building. An increase in CAES vessel size causes a slight increase in electricity price for a dramatic rise in building independence, therefore a large CAES vessel should be chosen if this trade-off is acceptable for the case in question. Overall, the SOFC/CAES system provides a cost-effective method if providing power and heat with near grid-independence is a main priority; however the system does not solve the inherent problem of distributed generation being an expensive method of heat and power production.

Chapter 6

CONLCUSIONS AND RECOMMENDATIONS

6.1. Conclusions

The objective of this work was to design an integrated SOFC/CAES system for the small (kW) scale, load-following distributed generation of heat, hot water, and power. A techno-economic analysis was desired for the application of the SOFC/CAES system for a building on the campus of McMaster University.

Chapter 2 provided a description of the models, simulated using Aspen Plus v8.0, used to determine the output of the integrated SOFC/CAES system. The rigorous models were then approximated using surrogate pseudo steady state models to significantly decrease the computational time associated with the annual load-following analysis. The surrogate models provided accurate predictions of the output of the SOFC/CAES system compared to the rigorous Aspen Plus simulations and were used in all subsequent analyses.

Chapter 3 discussed the implementation of the surrogate models in a generic GUI analysis tool. The purpose of this tool is to allow for the integrated SOFC/CAES system proposed in this research to be analysed in a wide variety of datasets and case studies. The tool allows the user to provide expected demand profiles for heat and power, as well as any additional renewable power supply that may be present for the building. The user is then able to provide information for the size and of their system, as well was a variety of performance characteristics, such as fuel utilization, degradation rate and inversion efficiency. The surrogate models are used to analyze the load-following capabilities of the system, with a primary focus on exactly meeting the power demand and not overproducing heat on an hourly basis. The GUI then provides a comprehensive set of metrics to assess the ability of the system to follow the demand profiles and analyze the size of the SOFC and CAES systems. The GUI also provides information on the CO_2 emissions of the system and compares it to the emissions associated with the building if all power was provided by a NGCC and all heat was provided by a high-efficiency furnace.

In Chapter 4, the GUI was used with the dataset for the proposed ExCEL building at McMaster University. The SOFC/CAES system was used in conjunction with on-site solar panels to deliver both power and heat to the building. The FU of the system was found to have a significant effect on system performance as a high (80%) FU results in a low TER and improves load-following performance in the hotter (summer/spring) months while a low (65%) FU results in a high TER and is superior in the colder (winter/autumn) months. A strategy in which the FU of the system is modified twice per year results in the best load-following performance as it provides a significant portion of both the heat (71.18%) and power (92.61%) demand for the building. All FU case studies of the SOFC/CAES system also reduce the emissions associated with the building compared to the state-of-the-art NGCC/furnace combination. The performance of the system was highly dependent on the size of the SOFC and moderately dependent on the size of the CAES vessel; however it was found that, overall, the SOFC/CAES system was able to adequately meet heat and power demand with a reduction in CO_2 emissions if it is properly sized.

Chapter 5 provided the economic analysis of applying the proposed SOFC/CAES system for the ExCEL building. The system was able to provide power and heat at a lower cost than other DG systems (such as diesel generator/furnace); however, as with all DG systems, the energy costs significantly higher than current market prices. The cost was sensitive to the size of the SOFC/CAES system, with a larger SOFC slightly reducing electricity cost until a certain threshold and a larger CAES providing a slight increase in cost.

Overall, this research demonstrates the promising potential of a novel SOFC/CAES system in providing heat, hot water, and power for a building on McMaster University in a load-following manner. Commercial buildings, such as small business offices, with similar demand profiles which require or desire grid-independence would likely benefit from the implementation of the SOFC/CAES system.

6.2. Recommendations for future work

There is a significant amount of work still required in order to prove the general application of such a system for distributed CHP generation.

1. Variety of Datasets

The general analysis GUI will be used with different power demand, heat demand, and renewable supply datasets to determine the applicability of the system on a more general basis, rather than specifically to the McMaster University case study presented in this work. These case studies can vary drastically in their demand trends, i.e. one dataset with a larger heat to power demand ratio (for somewhere such as northern Canada), and another dataset with nearly no heat demand (for a location such as Las Vegas). These studies are expected to show a more general applicability of the SOFC/CAES system in load-following CHP production.

2. System Optimization

The size of the SOFC and CAES components can be optimized to avoid consistent overproduction or underproduction. A multi-component optimization can be performed based on the user's desire to optimize certain metrics (CO_2 emissions, electricity price, percentage power demand met, etc.). This optimization can be programmed into the GUI, providing yet another feature for the analysis tool. Additionally, the timing for the FU changes for the MSFU system can be optimized using forecasted heat and power demands to minimize the mismatch between demand and supply rather than heuristically altering the FU at seasonal changes. This is anticipated to provide a better indication of the thermal electrical load-following benefits of the MSFU system.

3. Rolling Horizon Optimization

Nease and Adams demonstrated that the performance of a megawatt scale SOFC/CAES system can be improved by implementing a rolling horizon optimization (RHO) to compute system output based on predicted power demands (Nease & Adams II, 2014). A RHO can also be used for the small-scale CHP production, taking into account future heat and power demand predictions, as well as future renewable power supply predictions. The RHO is expected to improve the load-following performance of the system by avoiding completely emptying or completely filling the CAES vessel as much as possible.

List of References

Ackermann, T., Andersson, G. & Söder, L., 2001. Distributed generation: a defnition. *Electric Power Systems Research,* Volume 57, pp. 195-204.

Adams II, T. A. & Barton, P. I., 2010. High-efficiency power production from natural gas with carbon capture. *Journal of Power Sources,* Volume 195, pp. 1971-1983.

Adams II, T. A., Nease, J., Tucker, D. & Barton, P. I., 2012. Energy Conversion with Solid Oxide Fuel Cell Systems: A Review of Concepts and Outlooks for the Short- and Long- Term. *Industrial & Engineering Chemistry Research,* pp. 3089-3111.

Alanne, K. & Saari, A., 2006. Distributed energy generation and sustainable development. *Renewable & Sustainable Energy Reviews,* Volume 10, pp. 539-558.
Canada Plan Service, 2010. *Hot Water Heating.* [Online]

Available at: http://www.cps.gov.on.ca/english/plans/E9000/9735/M-9735La.pdf
[Accessed December 2014].

Duquette, J., Wild, P. & Rowe, A., 2014. The potential benefits of widespread combined hear and power based district energy networks in the province of Ontario. *Energy,* Volume 67, pp. 41-51.

Energy and Environmental Analysis, 2008. *Technology Characterization: Microturbines*

Energy Information Administration (EIA), 2012. *Voluntary Reporting of Greenhouse Gases Program.* [Online]
Available at: http://www.eia.doe.gov/oiaf/1605/coefficients.html
[Accessed December 2014].

Environment Canada, 2014. *Historical Weather Data - Hamilton*

Fang, Q. et al., 2015. SOFC stack performance under high fuel utilization. *International Journal of Hydrogen Energy,* Volume 40, pp. 1128-1136.

Fertig, E. & Apt, J., 2011. Economics of compressed air energy storage to integrate wind power: A case study in ERCOT. *Energy Policy,* 39(5), pp. 2330-2342.

Harun, N. F., Tucker, D. & Adams II, T. A., 2014. Fuel Composition Transients in Fuel Cell Turbine Hybrid for Polygeneration Applications. *Journal of Fuel Cell Science and Technology,* 11(6), pp. 061001-061009.

Hernandez-Pacheco, E. et al., 2004. A macro-level model for determining performance characteristic of solid oxide fuel cells. *Journal of Power Sources,* Volume 338, pp. 174-186.

Horizon Utilities, 2015. *Electricity Rates.* [Online]
Available at:
http://www.horizonutilities.com/myHome/ElectricityRates/Pages/default.aspx
[Accessed 5 February 2015].

Huijsmans, J. P., van Berkel, F. P. & Christie, G. M., 1998. Intermediate temperature SOFC - a promise for the 21st century. *Journal of Power Sources,* Volume 71, pp. 107-110.

IEC, 2007. *Efficient Electrical Energy Transmission and Distribution,* Geneva, Switzerland: International Electrotechnical Commission.

Ingram, G. K., 1998. Patterns of Metropolitan Development: What Have We Learned?. *Urban Studies,* 35(7), pp. 1019-1035.

Laosiripojana, N. & Assabumrungat, S., 2007. Catalytic steam reforming of methane, methanol, and ethanol over Ni/YSZ: The possible use of these fuels in internal reforming SOFC. *Journal of Power Sources,* Volume 163, pp. 943-951.

Nagel, F. P., Schildhauer, T. J. & Biollaz, S. M., 2009. Biomass-integrated gasification fuel cell systems - Part 1: Definition of systems and technical analysis. *International Journal of Hydrogen Energy,* Volume 34, pp. 6809-6825.

Nair, N.-K. C. & Garimella, N., 2010. Battery energy storage systems: Assessment for small-scale renewable energy integration. *Energy and Buildings*, Volume 42, pp. 2124-2130.

National Energy Technology Laboratory, 2013. *Assessment of the Distributed Generation Market Potential for Solid Oxide Fuel Cells,* s.l.: s.n.

Natural Resources Canada, 2012. *Heating with Gas.* [Online]
Available at:
http://www.nrcan.gc.ca/sites/www.nrcan.gc.ca/files/energy/pdf/energystar/Heating_With_Gas.pdf
[Accessed 5 February 2015].

Nease, J. & Adams II, T. A., 2013. System for peaking power with 100% CO2 capture by integration of solid oxide fuel cells with compressed air energy storage. *Journal of Power Sources,* Issue 228, pp. 281-293.

Nease, J. & Adams II, T. A., 2014. Application of rolling horizon optimization to an integrated solid-oxide fuel cell and compressed air energy storage plant for zero-emissions peaking power under uncertainty. *Computer and Chemical Engineering,* Volume 68, pp. 203-219.

Nease, J. & Adams II, T. A., 2014. Life cycle analyses of bulk-scale solid oxide fuel cell power plants. *Canadian Journal of Chemical Engineering.*

Nyboer, J., Bennett, M., Wolinetz, M. & Melton, N., 2014. *Cogeneration Facilities in Canada,* CIEEDAC.

Oak Ridge National Laboratory, 2011. *Biomass Energy Data Book Appendix A. Lower and Higher Heating Values of Gas, Liquid and Solid Fuels*.

Olesen, B. W., 2002. Radiant Floor Heating In Theory and Practice. *ASHRAE Journal,* 44(7), pp. 19-24.

Ontario Energy Board, 2015. *Natural Gas Rates.* [Online]
Available at:
http://www.ontarioenergyboard.ca/OEB/Consumers/Natural+Gas/Natural+Gas+Rates#prices
[Accessed 5 February 2015].

Panagopoulos, A. A., Chalkiadakis, G. & Koutroulis, E., 2012. *Predicting the Power Output of Distributed Renewable Energy Resources within a Broad Geographical Region.* Montpellier, France

Pepermans, G. et al., 2005. Distributed generation: definition, benefits and issues. *Energy Policy,* Volume 33, pp. 787-798.

Raftery, P., Lee, K. H., Webster, T. & Bauman, F., 2012. Performance analysis of an integrated UFAD and radiant hydronic slab system. *Applied Energy,* Volume 90, pp. 250-257.

Rosen, M., Le, M. & Dincer, I., 2005. Efficiency analysis of a cogeneration and district energy system. *Applied Thermal Engineering,* Volume 25, pp. 147-159.

Seider, W., Seader, J., Lewin, D. & Widagdo, S., 2009. *Product and Process Design Principles.* 3rd ed. Hoboken, NJ: John Wiley & Sons, Inc..

Solar Energy Industries Association, 2014. *Solar Energy Facts: Q3 2014,* s.l.: s.n.

Stiller, C., Thorun, B. & Bolland, O., 2006. Safe Dynamic Operation of a Simple SOFC/GT Hybrid System. *Journal of Engineering for Gas Turbines and Power*, 128(3), pp. 551-559.

Wang, R. Z., Yu, X., Ge, T. S. & Li, T. X., 2013. The present and future of residential refrigeration, power generation and energy storage. *Applied Thermal Engineering,* 53(1), pp. 256-270.

Williams, M. C., Strakey, J. P. & Singhal, S. C., 2004. U.S. dsitributed generation fuel cell program. *Journal of Power Sources,* Volume 131, pp. 79-85.

Williams, M. C., Strakey, J. P. & Surdoval, W. A., 2005. U.S. Department of Energy's Solid Oxide Fuel Cells: Technical Advances. *Applied Ceramic Technology,* 2(4), pp. 295-300.

Wolsink, M., 2012. The research agenda on social acceptance of distributed generation in smart grids: Renewable as common pool sources. *Renewable and Sustainable Energy Reviews,* Volume 16, pp. 822-835.